Mobility and Safety Impacts of Work Zone Lane and Shoulder Widths

Final Report
May 2024

SWZDI
Smart Work Zone Deployment Initiative

Sponsored by
Smart Work Zone Deployment Initiative
(Part of TPF-5(438))
Federal Highway Administration
(Part of InTrans Project 20-733)

About the Smart Work Zone Deployment Initiative

The Smart Work Zone Deployment Initiative (SWZDI) is a transportation pooled fund that supports research investigations into better ways to improve the safety and efficiency of traffic operations and highway work in work zones. The primary objective is to promote and support research and outreach activities that focus on innovative policies, processes, tools, and products that enhance the implementation, safety, and mobility impacts of work zones.

The preparation of this report was financed in part through funds provided by the Iowa Department of Transportation through its "Second Revised Agreement for the Management of Research Conducted by Iowa State University for the Iowa Department of Transportation" and its amendments.

Technical Report Documentation Page

1. Report No.	2. Government Accession No.	3. Recipient's Catalog No.
Part of TPF-5(438)		

4. Title and Subtitle	5. Report Date
Mobility and Safety Impacts of Work Zone Lane and Shoulder Widths	May 2024
	6. Performing Organization Code
7. Author(s)	**8. Performing Organization Report No.**
Madhav V. Chitturi, Glenn Vorhes, Zhaoxiang He, Boris Claros, Xiao Qin, Andrea R. Bill, and David A. Noyce	Part of InTrans Project 20-733
9. Performing Organization Name and Address	**10. Work Unit No. (TRAIS)**
University of Wisconsin-Madison 1415 Engineering Drive Madison, WI 53706 University of Wisconsin-Milwaukee NWQ 4414, P.O. Box 784 Milwaukee, WI 53201	**11. Contract or Grant No.**
12. Sponsoring Organization Name and Address	**13. Type of Report and Period Covered**
Smart Work Zone Deployment Initiative Iowa Department of Transportation 800 Lincoln Way Ames, Iowa 50010 Federal Highway Administration U.S. Department of Transportation 1200 New Jersey Avenue SE Washington, DC 20590	Final Report **14. Sponsoring Agency Code** Part of TPF-5(438)

15. Supplementary Notes

Visit https://swzdi.intrans.iastate.edu/ for color pdfs of this and other research reports.

16. Abstract

The goal of this project was to quantify the mobility and safety impacts of different combinations of lane width and shy distance to a barrier for a given paved width. The research team developed a device to measure lateral distance and derive speed, vehicle length/type, and headway information under day and night conditions. Data collected at 17 locations in Illinois, Michigan, and Wisconsin were used for the analyses. Lateral distance data of over a quarter of a million vehicles were used for the safety analysis. Extreme value theory (EVT) modeling was conducted to estimate the probabilities of right edge line encroachment and right barrier contact. Wider lanes were found to have decreased edge line encroachment and barrier contact, while wider shy distances were associated with increased edge line encroachment and decreased barrier contact. The speeds of over 125,000 free flow vehicles were used to quantify the mobility impact. Linear regression modeling was conducted to develop models for estimating free flow speeds in work zones. Work zone free flow speed increases with an increase in speed limit, lane width, and left/right shy distances to a barrier. A case study of a 55 mph posted work zone with two open lanes and barriers on both sides with an available paved width of 26 ft is presented. The results indicate that 11 ft lanes with 2 ft shy distances have a slightly lower probability of right barrier contact (for vehicles in the right lane) than 12 ft lanes with 1 ft shy distances while having a greater free flow speed. This research demonstrates how lateral distance can be collected and modeled along with speed data to assess safety and mobility impacts in work zones. Limitations of the study are acknowledged, and recommendations for future research are presented.

17. Key Words	18. Distribution Statement
lane width—safety—shoulder width—speed—work zone	No restrictions.

19. Security Classification (of this report)	20. Security Classification (of this page)	21. No. of Pages	22. Price
Unclassified.	Unclassified.	96	NA

Form DOT F 1700.7 (8-72) **Reproduction of completed page authorized**

Mobility and Safety Impacts of Work Zone Lane and Shoulder Widths

Final Report
May 2024

Principal Investigator
David A. Noyce, Professor
University of Wisconsin-Madison

Co-Principal Investigator
Xiao Qin, Professor
University of Wisconsin-Milwaukee

Research Assistant
Zhaoxiang He

Authors
Madhav V. Chitturi, Glenn Vorhes, Zhaoxiang He, Boris Claros,
Xiao Qin, Andrea R. Bill, and David A. Noyce

Sponsored by
Smart Work Zone Deployment Initiative and
Federal Highway Administration Pooled Fund Study TPF-5(438):
Iowa (lead state), Illinois, Kansas, Michigan, Missouri, Nebraska, Texas, and Wisconsin

Preparation of this report was financed in part
through funds provided by the Iowa Department of Transportation
through its Research Management Agreement with the
Institute for Transportation
(InTrans Project 20-733)

A report from
Smart Work Zone Deployment Initiative
2711 South Loop Drive, Suite 4700
Ames, IA 50010-8664
Phone: 515-294-8103 / Fax: 515-294-0467
https://swzdi.intrans.iastate.edu/

TABLE OF CONTENTS

LIST OF FIGURES

LIST OF TABLES

ACKNOWLEDGMENTS

This research was conducted under the Smart Work Zone Deployment Initiative (SWZDI) and Federal Highway Administration (FHWA) Pooled Fund Study TPF-5(438), involving the following state departments of transportation (DOTs):

- Iowa (lead state)
- Illinois
- Kansas
- Michigan
- Missouri
- Nebraska
- Texas
- Wisconsin

The authors would like to thank the FHWA, the Iowa DOT, and the other pooled fund state partners for their financial support and technical assistance. The Iowa DOT also used Federal SPR Part II, CFDA 20.205 funding for this work.

The authors would also like to thank the technical advisory committee (TAC) members for their technical assistance and the Illinois, Michigan, and Wisconsin DOTs for their support with the data collection efforts.

EXECUTIVE SUMMARY

Work zones need to be designed within a given paved width. This is especially the case when traffic is crossed over. The challenge faced by designers is in understanding the safety and mobility implications of the allocation of lanes and shy distances for a given paved width. No study has evaluated the safety and mobility impacts of combinations of lane widths and shy distances in work zones. For example, if a paved roadway width of 26 ft were available, would it be better to have two 12 ft lanes with 1 ft shy distances or two 11 ft lanes with 2 ft shy distances? Therefore, the goal of this project was to quantify the mobility and safety impacts of different combinations of lane width and shy distance to a barrier for a given paved roadway width.

Commercial devices for collecting vehicle speed are widely available, but none are available to measure the lateral distance of vehicles. The research team developed a device using two directional lidar sensors with update rates of 1,000 Hz (one reading every millisecond) to measure lateral distance. The data obtained can be used to derive vehicle speed, vehicle length/type, and headway information under day and night conditions. Data collected at 17 locations in Illinois, Michigan, and Wisconsin were used for the analyses. All of the locations had two open lanes in each direction in the work zone with concrete barriers on both sides. The lane widths were 11 or 12 ft, while the shy distances to the barriers ranged from 1 to 3 ft. Information about speed limit, enforcement or speed management strategies, and any other factors that could impact speed or lane position was noted. The data collection device was mounted on the right concrete barrier only because the traffic was counter-directional or the median side could not be safely accessed by the research team.

Vehicle’s lateral position in the right travel lane was used as a surrogate safety measure to understand the safety impact of lane width and shy distance. Lateral distance data of over a quarter of a million vehicles were used for the safety analysis. The safety analysis only considered right departures for vehicles in the right lane. Compared to the daytime, vehicles moved farther away from the edge line and barrier in the nighttime. Lane width and shy distance significantly influenced vehicles’ lateral distance in relation to the edge line and barrier. Vehicles tend to move farther from the edge line and the barrier in 12 ft lanes compared to 11 ft lanes. Vehicles tend to gravitate closer to the edge line but farther from the barrier with larger shy distances. Extreme value theory (EVT) modeling was conducted to estimate the probabilities of right edge line encroachment and right barrier contact. Wider lanes were found to have decreased edge line encroachment and barrier contact, while wider shy distances were associated with increased edge line encroachment and decreased barrier contact. The EVT models can be used to estimate the right edge line encroachment and right barrier contact probabilities for different combinations of lane width and shy distance.

Free flow speeds of over 125,000 vehicles were used to quantify the mobility impacts of lane width and shy distance. Unlike the safety analysis, which only considered vehicles in the right lane, the mobility analysis considered vehicles in both lanes. Linear regression modeling was conducted to develop two models for estimating free flow speeds in work zones based on geometric and operational variables. Both models indicate similar trends with respect to the impact of the various variables: work zone free flow speed increases with an increase in speed limit, lane width, and left/right shy distance to a barrier. Nighttime free flow speeds were higher than daytime free flow speeds, and speed feedback signs reduced the free flow speeds. Compared to Wisconsin, speeds were higher in Michigan and even higher in Illinois.

A case study of a 55 mph posted work zone with two open lanes and barriers on both sides with an available paved width of 26 ft is presented. The results indicate that 11 ft lanes with 2 ft shy distances have a slightly lower probability of right barrier contact (for vehicles in the right lane) than 12 ft lanes with 1 ft shy distances while having a greater free flow speed. This research demonstrates how lateral distance can be collected and modeled along with speed data to assess safety and mobility impacts in work zones. Limitations of the study are acknowledged, and recommendations for future research are presented.

1. INTRODUCTION

Aging infrastructure and increasing traffic volumes necessitate extensive work zones on the highway system. According to the National Work Zone Safety Information Clearinghouse, in 2021, 956 fatalities, about 42,000 injuries, and about 106,000 crashes occurred in work zones in the United States (NWSIC 2019). Furthermore, work zones contributed to 586 million hours of vehicle delay, which translates to $8.1 billion in user delay costs. Transportation agencies strive to mitigate the safety and mobility impacts of work zones using a variety of strategies as part of work zone transportation management plans. Closing one side of a divided multilane highway and crossing over traffic to the other side as a two-way operation is being used more frequently by transportation agencies. This strategy removes all traffic from the work area, thus reducing the exposure of workers to traffic, improves contractor control of the work area and work quality, and potentially reduces the duration of the work zone.

Work zones need to be designed within a given paved roadway width. This is especially the case with counter-directional flow when traffic is crossed over to opposing lanes. The challenge faced by designers is in understanding the safety and mobility implications of the allocation of lanes and shy distances for a given paved width. For example, if a paved width of 26 ft were available, would it be better to have two 12 ft lanes with 1 ft shoulder/shy distances or two 11 ft lanes with a 2 ft shoulder/shy distances? Narrower lanes would reduce speeds, which could reduce crash severity if a crash were to occur. On the other hand, (1) crash frequency could increase because of narrower lanes, and (2) reduced speeds could decrease capacity and increase the likelihood of back-of-queue crashes. A single study on two-lane roadways in non-work zone conditions examined the safety impacts of the tradeoff between lane and shoulder width. However, no study has evaluated the safety and mobility impacts of combinations of lane widths and shy distances in work zones.

The goal of this project was to quantify the mobility and safety impacts of different combinations of lane width and shy distance to a barrier for a given paved width. The rest of the report is organized as follows. Chapter 2 provides a review of state practices with regard to work zone lane width and shy distance and a summary of past research on the mobility and safety impacts of lane/shoulder width and shy distance in work zones. Chapter 3 describes the development of the data collection device, an algorithm for processing the data, validation of the device/algorithm, and the sites where data were collected. Chapters 4 and 5 present the safety and mobility analysis and modelling, respectively. Chapter 6 presents a case study comparing the safety and mobility estimates of two possible configurations of lane width and shy distance for 26 ft of paved width. Chapter 7 presents conclusions, limitations, and recommendations.

2. LITERATURE REVIEW

The research team conducted a literature review to document existing knowledge of the impacts of lane and shoulder widths on work zone mobility and safety. The following sections describe (1) state practices, (2) mobility impacts, and (3) safety impacts.

2.1. State Practices

NCHRP Report 581: Design of Construction Work Zones on High-Speed Highways documented state work zone design guidance following a survey of state departments of transportation (DOTs) (Mahoney et al. 2007). Since NCHRP Report 581 was published in 2007, the information may not be current. However, for the sake of completeness, the findings from NCHRP Report 581 are presented here.

2.1.1. Lane Width

Guidance on lane width from 22 state DOTs is summarized in NCHRP Report 581 as follows: "DOTs prefer that construction work zone travel lane widths meet the permanent road criteria for the affected facility. Several cases identified 12 ft as the desirable lane width. With varying degrees of stated reluctance, 14 states indicated using lanes as narrow as 10 ft under some circumstances." Many states require or generally use 11 ft for lane width on freeways/high-speed highways (Mahoney et al. 2007).

2.1.2. Shoulder Width

Eight states reported guidance for shoulder width on divided highways in NCHRP Report 581 (Mahoney et al. 2007), as summarized in Table 2-1.

Table 2-1. State DOT work zone shoulder width practices

State DOT	Left Shoulder Width (ft)	Right Shoulder Width (ft)
California	10	5
Connecticut	2	2
Illinois	2	2
Indiana	2	2
North Carolina	4[1]	4[1]
South Dakota	4[2]	
Virginia	10	
Wisconsin	2–3	2–3

[1] Minimum for crossover and detours associated with all functional classes; [2] Applies to median crossovers
Source: Mahoney et al. 2007

2.1.3. Barrier Offset

The AASHTO Green Book recommends that a 2 ft offset be provided where a roadside barrier, wall, or other vertical element adjoins the shoulder (AASHTO 2018). Chapter 9 of the AASHTO *Roadside Design Guide* also recommends a 2 ft offset to a portable concrete barrier (AASHTO 2011). According to NCHRP Report 581 (Mahoney et al. 2007), "[t]he DOTs of Alabama, Missouri and Nevada strive for offset barriers 2 ft from the traveled way. Virginia DOT reported that barriers are normally placed from 0.5 to 1 ft from the traveled way edge lines." The research team learned from conversations with work zone engineers in Michigan and Wisconsin that the general practice is to have the barriers at a 2 ft offset in their states.

2.2. Mobility Impacts

Limited research has been conducted on the impact of lane and shoulder widths on vehicle speeds in work zones. Chitturi and Benekohal (2005) examined the impact of lane and shoulder widths on speeds using field data from work zones. Traffic data were collected from 11 work zones on Interstate highways in Illinois in which one of the two lanes was open. The reductions in the free flow speeds of vehicles in work zones because of narrow lanes were higher than the reductions given in the *Highway Capacity Manual* for basic freeway sections. The narrower the lane, the greater the speed reduction, and the reduction in the free flow speeds of heavy vehicles was greater than the reduction in the free flow speeds of passenger cars. The authors recommended that 10.0, 7.0, 4.4, and 2.1 mph be used for speed reductions in work zones for lane widths of 10.0, 10.5, 11.0, and 11.5 ft, respectively.

Bham and Mohammadi (2011) studied the impact of reduced lane width using tubular markers at one work zone on I-44 in Rolla, Missouri. The work zone reduced the number of travel lanes from two to one and had a posted speed limit of 60 mph. However, the report does not state what the reduced lane width was. The reduced lane width resulted in a mean speed for cars and trucks of 4.0 and 8.1 mph less than the speed limit, respectively, during no construction activity. During construction activity, the mean speeds of cars and trucks were 8.5 and 11.1 mph less than the speed limit, respectively.

The 7th edition of the *Highway Capacity Manual* (TRB 2022) includes a formula for estimating free flow speeds in work zones, as shown in Equation 1. However, this formula does not account for lane or shoulder widths. The factors considered are work zone speed limit, ratio of work zone speed limit to non-work zone speed limit, lane closure severity, barrier type, day/night, and number of on-ramps/off-ramps.

$$FFS_{wz} = 9.95 + (33.49 \cdot f_{sr}) + (0.53 \cdot f_s) - (5.60 \cdot f_{lcsi}) \\ -(3.48 \cdot f_{br}) - (1.71 \cdot f_{dn}) - (1.45 \cdot f_{nr}) \quad (1)$$

where

FFS_{wz} = work zone free-flow speed (mph)

f_{sr} = speed ratio (decimal), i.e., the ratio of non-work zone speed limit to work zone speed limit
f_s = work zone speed limit (mph)
f_{lcsi} = lane closure severity index
f_{br} = barrier type (0 = concrete and hard barrier separation, 1 = cone, plastic drum, or other soft barrier separation)
f_{dn} = day/night (0 = daylight, 1 = night)
f_{nr} = number of on-ramps and off-ramps within three miles upstream and downstream of the work zone area

2.3. Safety Impacts

Graham et al. (1978) compared crash rates between projects that had reduced lane widths and projects that maintained normal lane widths. However, the level of lane width reduction was not mentioned. While the 6 projects with reduced lane widths experienced a 17.6% increase in crash rates, the other 69 projects with normal lane widths experienced a 6.6% increase. A study in Indiana used crash data from one long-term work zone and reported that increasing the inside and outside shoulder widths by 1 ft corresponds to 3.4% and 6.2% reductions in crashes, respectively (Tarko et al. 2011).

In the context of work zones, no research has examined the safety tradeoffs for different configurations of lane and shoulder widths given a fixed pavement width and number of lanes. However, this question has been examined in the context of conventional (non-work zone) two-lane highways. Research has examined the impact of narrower lanes and shoulders to provide additional travel lanes on freeways. The findings for conventional two-lane highways and freeways are presented here as a reference.

Gross et al. (2009) used geometric, traffic, and crash data from more than 52,000 miles of two-lane roadways in the states of Pennsylvania and Washington. A series of models were estimated for the most common pavement widths between 26 and 36 ft. In general, the crash modification factors (CMFs) developed indicate a slight benefit to increasing the lane width compared to the shoulder width for a fixed total width. Other salient findings are as follows:

- Shoulder width. Lane width has a greater effect on safety; as lane width increases, the effect of shoulder width decreases.
- Lane width. An increase in lane width does not always improve safety, especially with wider shoulders.

The Federal Highway Administration (FHWA) published a primer on the use of narrow lanes and narrow shoulders to improve capacity within an existing roadway footprint and reported favorable safety impacts. The primer reported a case study in Milwaukee, Wisconsin, that estimated that narrow lanes and shoulders would improve safety and reduce crashes using analyses based on the FHWA's *Highway Safety Manual*. A case study from Washington state, which used narrow lanes to accommodate part-time shoulder use, found that the crash rate decreased from 1.00 crashes per million vehicle miles traveled (MVMT) to 0.82 crashes per MVMT.

Urbanik and Bonilla (1987) studied the safety impacts of removing inside shoulders for use as travel lanes at 12 locations in California. A simple before-after comparison of crash rates was conducted. In all but one location, a nonsignificant change or a significant reduction in overall crashes was found. Crash severity was also not impacted. The authors ascribe the reduction in crash rates to reduction in congestion.

Bauer et al. (2004) examined the safety effects of narrow lanes and shoulder-use lanes to increase capacity of urban freeways. An empirical Bayes analysis was conducted using data from 124 sites in California. While conversions from four lanes to five lanes resulted in a 10% to 11% increase in crash frequency, conversions from five to six lanes resulted in smaller increases. Dixon et al. (2015) collected geometric, operational, and safety data from urban freeways in three cities in Texas (Dallas, Houston, and San Antonio) to study the safety effects of changes in lane/shoulder widths. Keeping the paved width constant, the adverse effect of reducing shoulder widths outweighed the safety benefits of an increased number of lanes.

2.4. Summary

Many states require or generally use 11 ft lane widths on freeways/high-speed highways. Minimum shoulder widths and barrier offsets are 2 ft in work zones. The *Highway Capacity Manual* does not incorporate lane and shoulder widths in free flow speed estimations (TRB 2022). Limited research has examined/quantified the impact of narrower lanes/shoulders in work zones. The findings suggest that the narrower the lane, the lower the free flow speeds. No research has examined the safety tradeoff among different configurations of lane and shoulder widths for a fixed pavement width and number of lanes. In the context of two-lane highways, a slight benefit to increasing the lane width compared to the shoulder width for a fixed total width was reported. A comprehensive analysis of mobility and safety impacts of different configurations of lane and shoulder width for a fixed pavement width is needed.

3. DATA COLLECTION

The research team built a device to measure the lateral position of vehicles and developed and validated an algorithm to compute vehicle speed, length, and headway. The device was used to collect data at over 20 locations in Illinois, Michigan, and Wisconsin. This chapter describes (1) the data collection device, (2) algorithm development, (3) validation of the data collection device/algorithm, and (4) study locations.

3.1. Data Collection Device

Devices for collecting vehicle speed using a variety of technologies, such as radar and light range detection, are widely available. No commercially available device was available to measure the lateral distance of vehicles as they pass through the detection field in a work zone. The research team developed a device using two directional lidar sensors with update rates of 1,000 Hz (one reading every millisecond) that can measure lateral position. The data obtained can be used to derive speed, vehicle length/type, and headway information under day and night conditions. The function is analogous to traffic detection with two pneumatic tube counters or two inductive loops. However, unlike tube sensors/inductive loops, which can only detect presence or absence, this configuration offers lateral distance measurements and eliminates the need for placement within the roadway. A diagram and a picture of the device deployed in a work zone are shown in Figure 3-1.

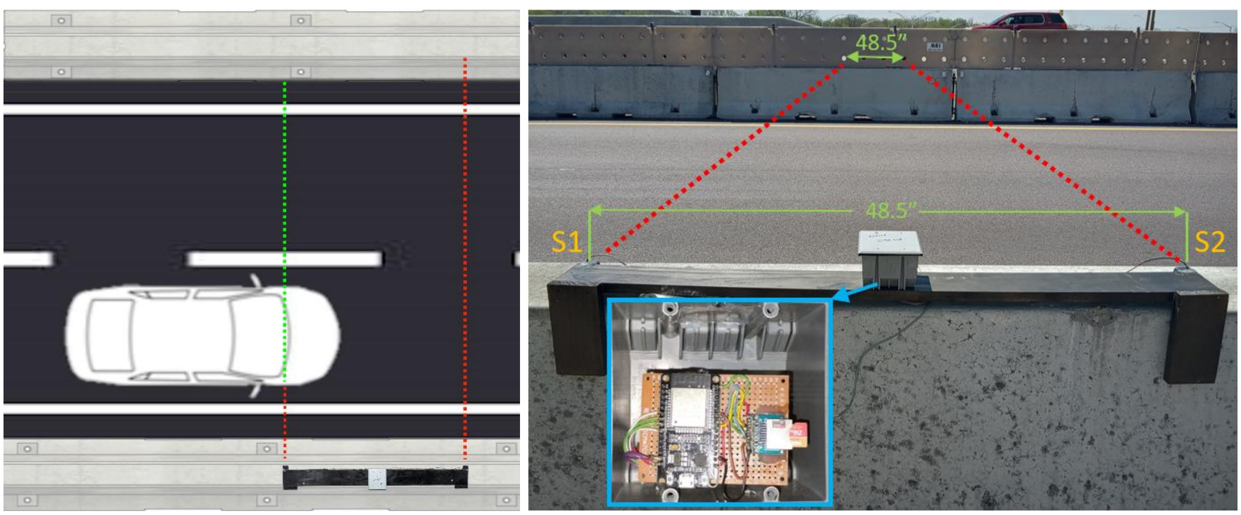

Figure 3-1. Schematic diagram and picture of data collection device in a work zone

The device consists of two directional lidar units, a microcontroller, and an SD card interface. The term "detector" will refer to the unit as a whole, and the term "sensor" will refer to the individual lidar units. While lidar can invoke the idea of point clouds from 3D scanners, the units used in this project functioned as one-directional range finders. Two Benewake TFmini plus lidar sensors were selected for the detector; each sensor has a configurable update rate of up to 1,000 Hz, a distance resolution of 1 cm, and a manufacturer-provided maximum range of about 40 ft (12 m). However, the stated maximum range is for ideal conditions with low ambient light. The effective range was expected to be lower but sufficient for detection of vehicles in the far lane at around 20 ft. The two lidar units were affixed to a structure to ensure parallel detection beams at 48.5 in. apart and to allow easy and secure placement on concrete Jersey barriers. The microcontroller received input from the lidar sensors and maintained a timestamp relative to the power-on time of the device. Finally, an SD card interface was used to record data as a comma-separated value (CSV) file, where each row held the timestamp in milliseconds and the lateral distance measurements for each sensor. The low power requirements of the components allowed the collection of data for up to 48 hours using 20,000 mAh power banks.

In addition to the device data collection, video was recorded at the study locations with the field of view showing the device and passing vehicles. The time the device was powered on is visible in the video to allow for synchronization with the recorded data. Up to one hour of video was recorded, and this proved to be sufficient for development and validation of the algorithm.

3.2. Algorithm Development

Vehicle information was extracted from the raw data consisting of rows with timestamps and the corresponding lateral distance measurements at the two sensors. With the flow of traffic, many combinations of vehicles could be encountered. The simplest case is where one vehicle is detected in either the near or the far lane. These cases would be expected to be visible in the data as square waves in the values of Sensors 1 and 2 as the vehicle is first detected at Sensor 1 at the leading edge of the vehicle, then at Sensors 1 and 2, and finally only at Sensor 2 as the vehicle's trailing edge passes the device detection field. Other combinations of vehicles occur as well. Figure 3-2 shows the expected permutations of vehicles in the near and far lanes.

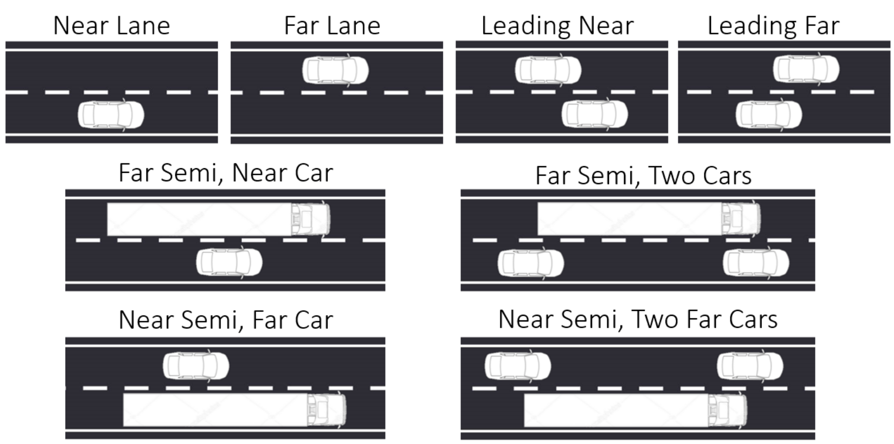

Figure 3-2. Permutations of vehicles observed in the field

The first step in algorithm development was to generate flag and signal values with which to identify vehicles and lane position scenarios. The original data sets for each location consisted of CSV files of up to several gigabytes depending on the duration of collection. To overcome the data size challenges, the data were loaded into a database where each row contained only records for which a valid lateral measurement was found for either Sensor 1 or 2, and a unique identifier for the location site was added. Further processing involved loading the data for each site into a pandas (Python Data Analysis Library) DataFrame.

Flag values were generated to identify transitions such as leading and trailing edges or the appearance of adjacent vehicles. In practice, the recorded data had intermittent gaps of generally 4 to 5 milliseconds in time. This behavior was identified early in the project and is due to periodic flushing of data from the microcontroller to the SD card. Though not a critical factor for the study, the no-data rows presented an additional challenge for algorithm development. Flag columns and reference values were generated for each row to indicate whether there was a measurement for Sensor 1 and Sensor 2. A separate column indicated whether each sensor value was within the expected minimum and maximum values for vehicles in either lane, a vehicle in Lane 1 (right lane), and a vehicle in Lane 2 (left lane), with reasonable lookahead and lookback time thresholds to fill in rows for which there were no data for either sensor. Further combining these flag values allowed assessment of each combination, i.e., whether the Sensor 1 and/or Sensor 2 data were within the expected minimum and maximum values for any vehicle in either lane, a vehicle in Lane 1, or a vehicle in Lane 2. It is with the extents of the flag values that the vehicle entities were identified and with which attributes such as lateral distance, speed, length, and vehicle classification were generated. An additional column was generated as the 30-millisecond period rolling average of the difference between the values at Sensor 2 and Sensor 1. Originally intended to identify the leading and trailing edges of vehicles, this value when graphed provided a visual indicator of transitions in the data as vehicles pass or adjacent vehicles appear.

Figure 3-3 shows the different conditions encountered in the data, starting with the simple cases of single vehicles in the near or far lane. The device is visible in the video screen capture images of the concrete barrier. Note the no-data and out-of-range reference values of 800 and 780, respectively, and the Sensor1/2, Lane 1 and Lane 2, and/or flag values. More involved examples include a leading vehicle in the near lane followed by an adjacent vehicle in the far lane and a leading vehicle in the far lane followed by an adjacent vehicle in the near lane. A far more complicated example is shown at the end, where a leading vehicle in the far lane is trailed by a semi in the near lane and a second vehicle in the far lane is detected under the trailer of the semi. Cases such as this were disregarded in the output because there is ambiguity in how many vehicles might be present. However, it was expected and addressed in the algorithm that semis could have a signature of detection of the tractor portion followed by a gap under the trailer and a short detection of the trailer wheels. These cases were handled by a special case wherein the output would report a single long vehicle.

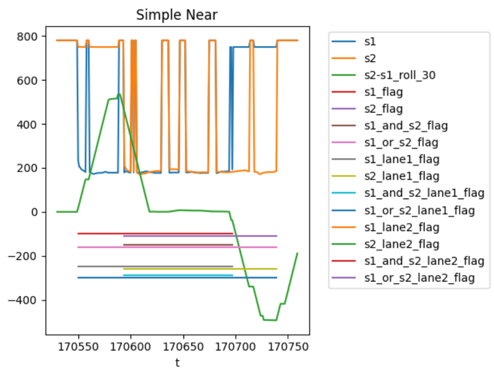
Simple Near
800
600
400
200
0
−200
−400
170550 170600 170650 170700 170750
t
s1
s2
s2-s1_roll_30
s1_flag
s2_flag
s1_and_s2_flag
s1_or_s2_flag
s1_lane1_flag
s2_lane1_flag
s1_and_s2_lane1_flag
s1_or_s2_lane1_flag
s1_lane2_flag
s2_lane2_flag
s1_and_s2_lane2_flag
s1_or_s2_lane2_flag

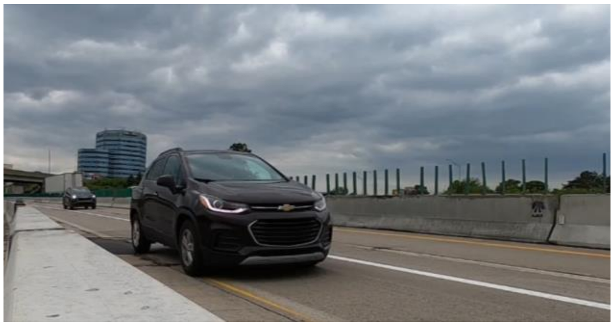

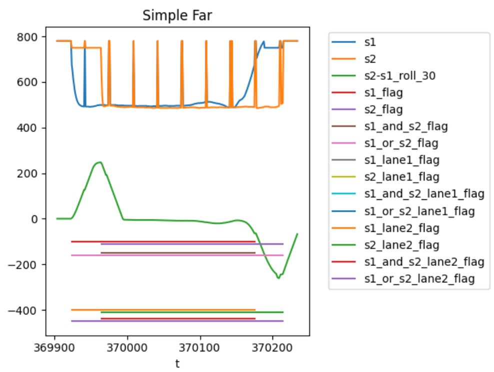
Simple Far
800
600
400
200
0
−200
−400
369900 370000 370100 370200
t
s1
s2
s2-s1_roll_30
s1_flag
s2_flag
s1_and_s2_flag
s1_or_s2_flag
s1_lane1_flag
s2_lane1_flag
s1_and_s2_lane1_flag
s1_or_s2_lane1_flag
s1_lane2_flag
s2_lane2_flag
s1_and_s2_lane2_flag
s1_or_s2_lane2_flag

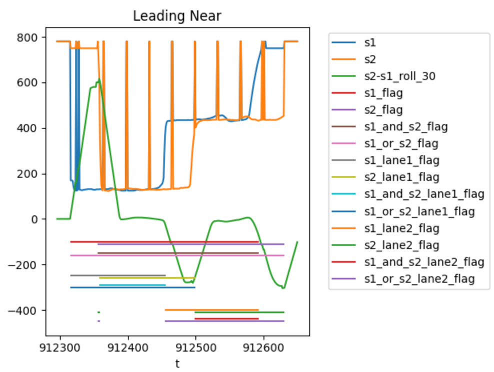
Leading Near
800
600
400
200
0
−200
−400
912300 912400 912500 912600
t
s1
s2
s2-s1_roll_30
s1_flag
s2_flag
s1_and_s2_flag
s1_or_s2_flag
s1_lane1_flag
s2_lane1_flag
s1_and_s2_lane1_flag
s1_or_s2_lane1_flag
s1_lane2_flag
s2_lane2_flag
s1_and_s2_lane2_flag
s1_or_s2_lane2_flag

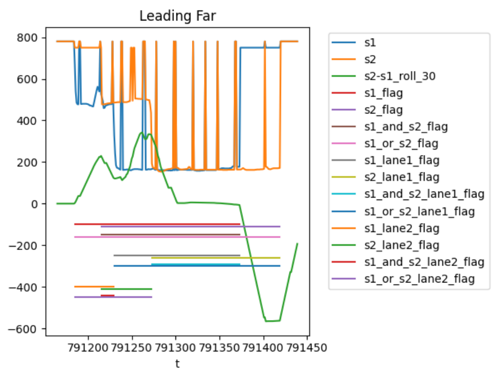
Leading Far
800
600
400
200
0
−200
−400
−600
791200 791250 791300 791350 791400 791450
t
s1
s2
s2-s1_roll_30
s1_flag
s2_flag
s1_and_s2_flag
s1_or_s2_flag
s1_lane1_flag
s2_lane1_flag
s1_and_s2_lane1_flag
s1_or_s2_lane1_flag
s1_lane2_flag
s2_lane2_flag
s1_and_s2_lane2_flag
s1_or_s2_lane2_flag

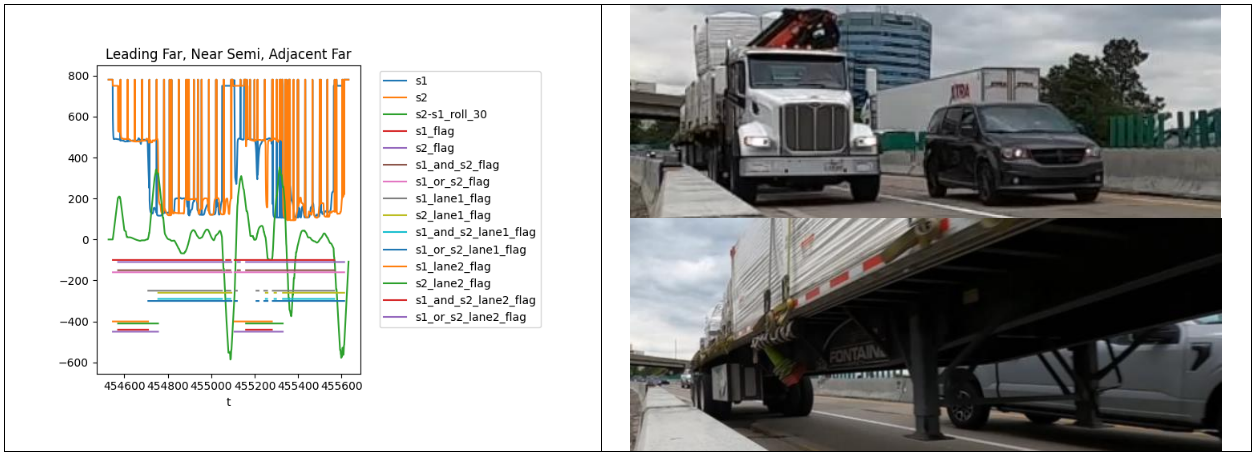

Figure 3-3. Data and pictures representing different permutations of vehicles observed in the field

The algorithm produced a multitude of attributes for each vehicle. The first attribute is the type of record, as seen in the previous examples. The record type is indicated as Simple when a vehicle is presented in either lane as LeadingNear or LeadingFar, where the leading vehicle is in the near or far lane, respectively. In the leading cases, a portion of the vehicle in the far lane is occluded, so a limited number of attributes can be calculated. In these cases, the attributes for the far vehicle are present in the same output row rather than being provided as a separate entity. The timestamp in milliseconds relative to the power-on time of the device is given as the time of the first measurement at Sensor 1 to the last measurement at Sensor 2.

Lateral distance statistics used the collection of measurements from both sensors. A vehicle was detected first by Sensor 1 and detected continuously until the trailing edge passed. Similarly, detection at Sensor 2 started some small duration after the start at Sensor 1. For much of the detection, there are measurements at both sensors. The number of potential measurements (rows) is as follows:

$$Row\ Count = \left(T_{S_1,last} - T_{S_1,first}\right) + \left(T_{S_2,last} - T_{S_2,first}\right) \quad (2)$$

where T is the time in milliseconds.

The number of valid measurements (values within the expected range) was given as s1_s2_count. The union of measurements for Sensors 1 and 2 were used to calculate the summary statistics. Preconditions were used to determine in which lane the vehicle was passing. Additional filters were used to limit the measurements to those with the expected values for a given lane.

This arrangement of two parallel detection beams presented two opportunities to calculate the speed: once at the leading edge and once at the trailing edge of the vehicle. As the vehicle passed, it was first detected by the upstream sensor designated by Sensor 1 and then a small but measurable time later at Sensor 2. Given the time difference, the known distance between the two sensors, and simple unit conversions, the speed of the vehicle based on the leading edge was calculated as follows:

$$Speed\ (mph) = \frac{48.5\ in}{(T_{S_2} - T_{S_1})\ sec} \cdot \frac{1\ mi}{63{,}360\ in} \cdot \frac{3{,}600\ sec}{1\ hr} \tag{3}$$

where T_{S_2} and T_{S_1} are the times of the first valid lateral distance measurement at Sensors 2 and 1, respectively, with units in seconds. Similarly, the speed of the vehicle based on the trailing edge was calculated with the same equation, but T_{S_2} and T_{S_1} were the times of the last valid lateral distance measurement at Sensors 2 and 1. A challenge with the device was that speed calculations were highly sensitive to the quality of data collection at the leading and trailing edges of vehicles. Small timing differences due to SD card flushing, no-data conditions, or missed measurements, particularly in the far lane, could lead to inconsistent speed measurements. A comparison column of the difference in the speeds calculated from the leading and trailing edges was generated. This provided a metric where lower percent differences represented vehicles with more reliable speed calculations. Given that tens of thousands of vehicles were detected at each location, the ability to reliably measure speed for even a fraction of the vehicles resulted in sufficient sample sizes. This is elaborated upon in Chapter 5.

The time difference between the first and last valid lateral distance measurements at Sensors 1 and 2 were similar if not identical because there would typically be very little change in speed over the roughly 4 ft detection zone during free flow conditions. The length of the vehicle was calculated using the previously generated speeds using the following:

$$T_{OccAve} = \frac{(T_{S_1,last} - T_{S_1,first}) + (T_{S_2,last} - T_{S_2,first})}{2} \tag{4}$$

$$Length\ (ft) = T_{OccAve} \cdot \frac{Speed\ mph}{hr} \cdot \frac{1\ hr}{3{,}600\ sec} \cdot \frac{5{,}280\ ft}{1\ mi} \tag{5}$$

where $T_{S_x,last}$ and $T_{S_x,first}$ are the times in seconds since powering on the device of the last and first valid lateral measurements at Sensor X (1 or 2), respectively; T_{OccAve} is the average occupied time; and the vehicle speed is in miles per hour. The calculation for vehicle length was done using both the leading and trailing edge speeds. Because the vehicle length and classification were derived from the calculated speed, these properties were similarly sensitive to measurement quality at the leading and trailing edges of the vehicles.

Additional columns were populated for LeadingNear and LeadingFar type records. Because a portion of the far vehicle was occluded by the near vehicle, lateral distance statistics such as the count, mean, standard deviation, minimum, and maximum only represented the portion of the far vehicle that was “visible” to the detector. The speed of the far vehicle was provided based on the vehicle edge available to the detector, i.e., the trailing edge for LeadingNear and leading edge for LeadingFar.

Because the speeds for the individual vehicles were highly sensitive to the measurements at the leading or trailing edges of those vehicles, a generalized average speed by lane was generated with which to generate vehicle length and classification. The “occupied” duration was much less sensitive to noise in the data, and use of the average speed allowed for a complement of the length and classification results. The average speed for a lane was the average of the average speeds for vehicles passing one minute before or after the row and was limited to those vehicles for which the difference between the leading and trailing speeds was less than 10%. The average speed in Lane 2 was further limited to vehicles within 20 mph of the average speed in Lane 1 to exclude those vehicles for which the speed difference was less than 10% but whose speeds were outside what would be expected. A count of the number of vehicles contributing to the average lane speed was provided.

Finally, each vehicle had a headway attribute determined as the time from the leading edge of the vehicle to the time of the leading edge of the previous vehicle in the same lane, with units in seconds.

3.3. Evaluation of Data Collection Device and Algorithm

The suitability of the device and algorithm were evaluated prior to deployment at the study locations. The device was deployed on a roadside barrier, with a GoPro capturing video of the device’s zone of detection configured to record at 240 frames per second. Traffic was sufficiently sparse to allow for making chalk marks on the pavement at 6 in. intervals relative to the lane marking. Figure 3-4 shows the field setup for the evaluation. This addressed challenges posed by previous validation attempts with unreliable lateral distance assessments in the video due to the inherently oblique angles. The chalk marks with known distances to a reference point allowed for accurate assessments of the lateral distance of the validation vehicles. The length of the middle lane marking was measured as well to serve as a reference to calculate vehicle speeds given the known time change between video frames of 1/240th of a second. During collection of the evaluation data, the location had a full shoulder open and the left lane was closed.

Figure 3-4. Field setup for evaluating data collection device

The lateral differences determined from the video compared very well with the measurements from the device. As mentioned previously, the value for the lateral distance of the vehicle was the average of the values taken from both sensors as the vehicle passed through the device's zone of detection. This gave hundreds of measurements resulting in a high confidence in the results, especially given the typically low standard deviations in a range of less than 10 cm. Figure 3-5 shows a comparison of lateral distances for the 134 vehicles as derived from the video and the processing algorithm. Table 3-1 shows the statistics for the lateral distance comparison. The mean difference was 5.1 in., with a minimum difference of 2.6 in. and a maximum difference of 6.9 in. Given that the chalk marks were placed at 6 in. intervals, the lateral distance estimate from the video could have an error of 1.5 in.

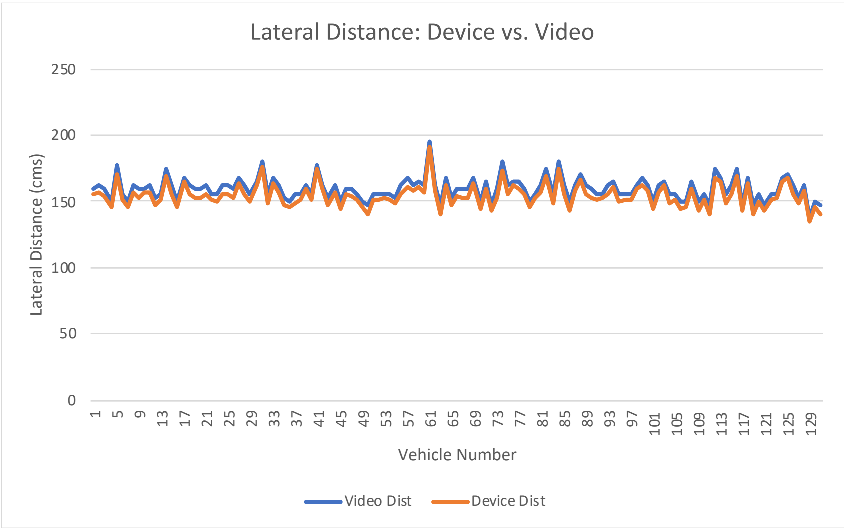

Figure 3-5. Comparison of lateral distances from the device and video

Table 3-1. Difference in lateral distance between the device and video

Count (veh)	Min (in.)	Mean (in.)	Max (in.)	SD[1] (in.)
134	2.6	5.1	6.9	1.2

[1] SD = standard deviation

Similar to the lateral distance evaluation, speeds for the 134 vehicles were derived from the video given the known length of the lane marking and the time difference between video frames. The speed comparison is shown in Figure 3-6.

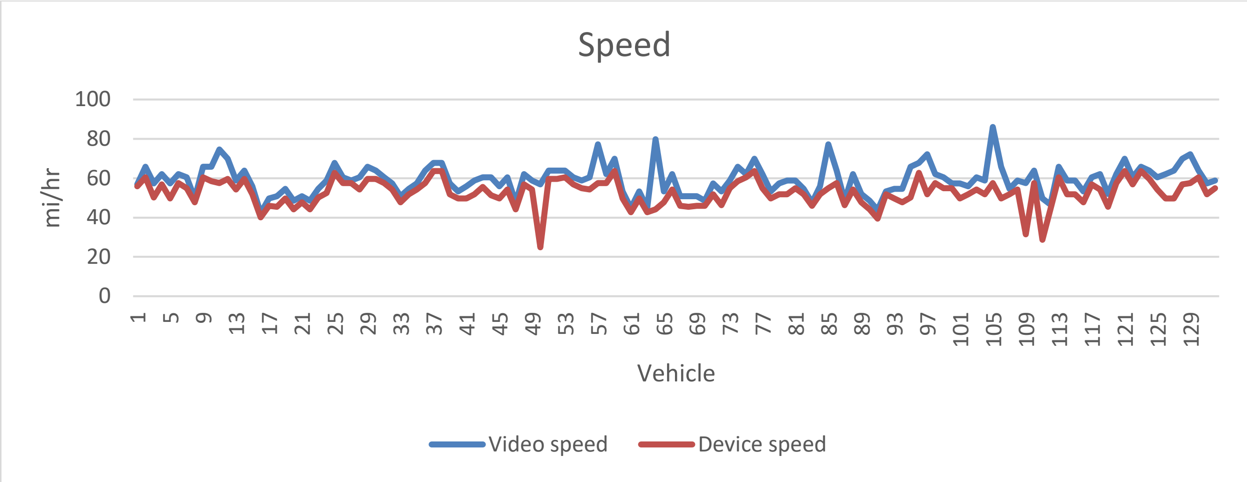

Figure 3-6. Comparing speeds from the device and video

Table 3-2 shows that the mean difference was 6.6 mph, with a minimum difference of 0.9 mph and a maximum difference of 35.7 mph. Oblique angles relative to the sensor at the curved leading and trailing edges of the vehicles resulted in less reliable measurements. As the vehicle progressed through the detection zone, the reflection improved as the surface became more consistently perpendicular to the sensor and the reflected signal became strong enough to be detected. Given that the distance between the two detectors was traveled in under 50 milliseconds at freeway speeds, a loss of a few readings could result in a large difference in speeds. Variations in measurement quality at the leading and trailing edges of the vehicles presented an obstacle for calculating speed. Additional checks to compare the speeds derived from the leading and trailing edges of the vehicles as well as with the speeds of temporally adjacent vehicles helped identify those records for which the speed was reliable. The large sample size provided a substantial number of records for which the speed calculations were considered reliable.

Table 3-2. Difference in speed between the device and video

Count (veh)	Min (mph)	Mean (mph)	Max (mph)	SD[1] (mph)
134	0.9	6.6	35.7	5.7

[1] SD = standard deviation

3.3.1. Evaluation Summary

The device performed well for an assessment of lateral distances, as demonstrated by the correlation of distances obtained from the video and the device. The average lateral distance was based on hundreds of individual measurements, with standard deviations typically below 5 cm (2 in). Derivation of speeds from the device proved to be more challenging. The sensors used for the device were nearing their functional limit in high ambient light conditions at distances for vehicles in the far (median side) lane. Given these concerns, each vehicle had a leading and trailing edge speed comparison. The high-quality records were identified as those for which the differences were small, indicating good capture of the measurements at both vehicle edges.

3.4.Study Locations

The number of combinations of lane width, shoulder width, number of lanes within the work zone, and barrier types would be enormous. Therefore, the technical advisory committee (TAC) members for this project directed the research team to focus on work zones with two open lanes, a barrier on either side, and a shy distance to the barrier of 1 or 2 ft. The TAC members provided the research team with work zones that met these criteria. The research team worked with the TAC members and individual project engineers to coordinate the field data collection. Data were collected at 20 locations across Illinois, Michigan, and Wisconsin. Due to data logging failure or a sensor being down, data were not available at 3 locations. Figure 3-7 shows a map of the 17 locations (from 7 work zone projects) across Illinois, Michigan, and Wisconsin where data were collected and used for analysis.

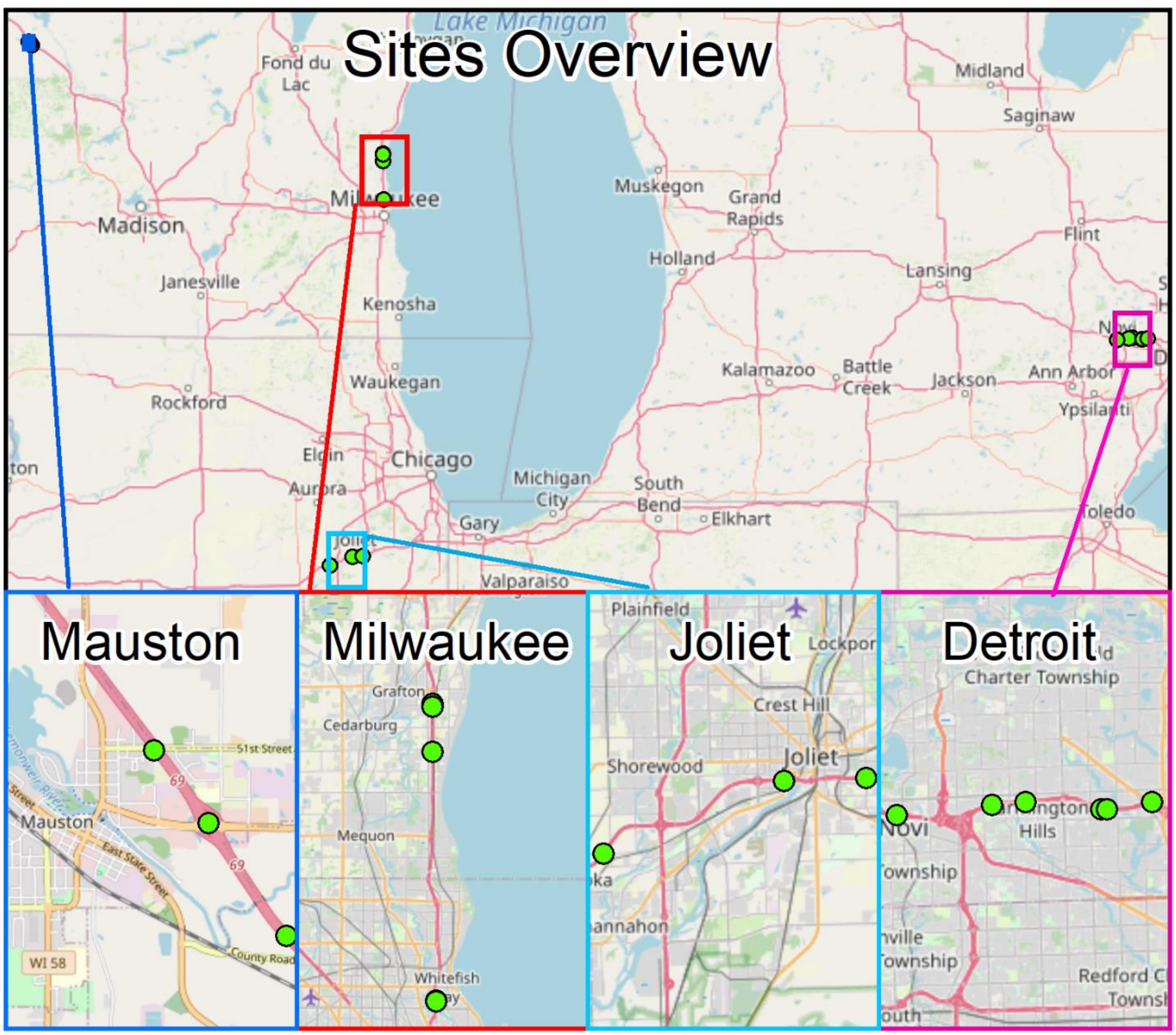

Figure 3-7. Map of data collection locations

The attributes of these locations are shown in Table 3-3. All of the locations had two open lanes in the work zone. The number of lanes outside the work zone varied from two to four. All but three locations had counter-directional flow (with the traffic crossed over to the opposing side) separated by concrete barriers with glare screens. All of the locations had concrete barriers on both sides, with shy distances to the barriers ranging from 1 to 3 ft. The data collection device was mounted on the right concrete barrier, as shown in Figure 3-1, for nearly two days. During the data collection, video data were recorded for up to an hour at each location. Information about speed limit, enforcement or speed management strategies, and any other factors that could impact speed or lane position was noted. Additionally, photographs of the views upstream and downstream of the device as well as the pavement were captured and are presented in the appendix. The actual shy distance to the right barrier from the edge of the pavement marking was measured in the field. The device could only be mounted on the shoulder because the traffic was counter-directional or the median side could not be safely accessed by the research team. The Mauston work zone (Locations WI-2, WI-3, and WI-4) used speed feedback signs on the approach to the work zone in both directions. None of the work zones had speed enforcement. All of the locations with 1 ft shy distances were very short sections (a few hundred feet), and that could have impacted the findings.

Table 3-3. Attributes of work zone data collection locations

Location	Nearest Big City	Description	Longitude	Latitude	Roadway Alignment	Lanes in Work Zone	Lanes Outside Work Zone	Speed Limit (mph)	Lane Width (ft)	Left Planned Shy Distance (ft)	Right Planned Shy Distance (ft)	Right Measured Shy Distance (in.)	Pavement Quality	Uneven Lanes	Counter-Directional Flow	Glare Screen	Date Device Placed
WI-1	Milwaukee, WI	I-43 URT NB	-87.91742	43.10949	Tangent	2	3	55	11	1	1	12	Poor	Right	Yes	Yes	10/19/22
WI-2	Mauston, WI	I-90/94 WB CTH N	-90.04694	43.78658	Curve[1]	2	2	60	11	2	2	19	Good	None	Yes	Yes	5/12/23
WI-3	Mauston, WI	I-90/94 WB WI 82	-90.05672	43.79679	Tangent	2	2	60	11	2	2	24	Good	None	Yes	Yes	5/12/23
WI-4	Mauston, WI	I-90/94 EB CTH G	-90.06359	43.80336	Tangent	2	2	60	12	2	3	33	Good	Right	Yes	Yes	5/12/23
WI-5	Milwaukee, WI	I-43 URT NB	-87.91742	43.10949	Tangent	2	3	55	11	1	1	14	Good	None	Yes	Yes	5/16/23
WI-6	Milwaukee, WI	I-43 EXP NB 89.4	-87.92096	43.27862	Curve[1]	2	2	60	12	2	2	24	Ok	Both	Yes	Yes	5/16/23
WI-7	Milwaukee, WI	I-43 EXP SB STH 60	-87.92060	43.31107	Curve[1]	2	2	60	12	2	2	32	Good	None	Yes	Yes	5/16/23
WI-8	Milwaukee, WI	I-43 EXP SB STH 60	-87.92058	43.30917	Tangent	2	2	60	12	2	2	34	Good	None	Yes	Yes	5/16/23
MI-1	Detroit, MI	I-96 EB Novi	-83.48026	42.48734	Tangent	2	3	60	11	2	3	30	Ok	Left	Yes	Yes	6/14/23
MI-2	Detroit, MI	I-696 EB Halsted	-83.41077	42.49296	Curve[1]	2	4	60	11	2	2	22	Ok	Both	Yes	Yes	6/14/23
MI-3	Detroit, MI	I-696 EB Farmington	-83.38622	42.49469	Tangent	2	4	60	11	2	2	28	Ok	Both	Yes	Yes	6/14/23
MI-4	Detroit, MI	I-696 EB Middlebelt	-83.33105	42.49070	Curve[2]	2	4	60	11	2	2	22	Ok	None	Yes	Yes	6/14/23
MI-5	Detroit, MI	I-696 EB Middlebelt	-83.32688	42.49063	Tangent	2	4	60	11	2	2	22	Ok	None	Yes	Yes	6/14/23
MI-6	Detroit, MI	I-696 EB Telegraph	-83.29377	42.49437	Curve[3]	2	3	60	11	2	2	24	Poor	Both	Yes	Yes	6/14/23
IL-1	Joliet, IL	I-80 EB Wheeler	-88.10500	41.51168	Tangent	2	2	45	11	2	2	24	Ok	Right	No	No	10/17/23
IL-2	Joliet, IL	I-80 EB Briggs	-88.04276	41.51301	Tangent	2	2	45	12	3	1	13	Ok	None	No	No	10/17/23
IL-3	Joliet, IL	I-80 WB Briggs	-88.24125	41.47034	Tangent	2	2	45	12	3	1	13	Ok	None	No	No	10/17/23

4. SAFETY ANALYSIS

Safety data collection and modeling have been a challenge in the context of work zones. Crashes are rare events, thankfully, and therefore do not provide sufficiently robust results in situations such as work zones to use a crash history approach. Simulator-based approaches are hard to validate, and even the large-scale Second Strategic Highway Research Program (SHRP2) Naturalistic Driving Study (NDS) provided only several hundred traversals through work zones (Hallmark et al. 2021). Alternatively, traffic conflicts (e.g., number of encroachment events) could be considered because conflicts are more frequently observed than crashes. The encroachment-based approach has been commonly applied to develop relationships between roadside crashes and roadside conditions (Miaou 1997, Mak and Sicking 2003). Encroachment data, however, are not readily available, either. Tire track skid marks are often used when direct encroachment observations are not available.

Given the challenges of collecting encroachment data, vehicles' lateral position in a travel lane could serve as a surrogate safety measure and is critical to understanding the safety impact of lane width and shy distance. Therefore, the research team used the data collection device to collect large-scale lateral distance data at several work zones.

This chapter describes data processing, an exploratory data analysis of lateral distance data, the analysis and modeling methodology used, the modeling of lateral distance data, and finally an estimation of the probabilities of edge line encroachment and barrier contact.

4.1. Data Processing

Lateral distance (from the right side of the vehicle) was used as a surrogate safety measure to evaluate the probability of edge line encroachment or barrier contact within the work zones. Vehicles' lateral position data were gathered from 17 different locations. As explained in Section 3.2, for every vehicle, the mean and standard deviation of the lateral distance measured at the two sensors were computed. Records with large standard deviations of lateral distance (a standard deviation greater than 80 cm or 31.5 in) were considered as outliers and excluded from the data analysis.

As explained in Section 3.4, the research team collected lateral distance from the right side of each vehicle only. Consequently, the safety analysis was limited to lane departures in the right lane (Lane 1). All 17 locations had two lanes open in the work zone. Figure 4-1 illustrates the approach used to assign a lane to each vehicle. A passenger car was assigned to the right lane (Lane 1) if its lateral distance was less than or equal to (LW - 42) in., where LW is the lane width; otherwise, it was assigned to the left lane (Lane 2). A truck was assigned to right lane (Lane 1) if its lateral distance was less than or equal to (LW - 51) in.; otherwise, it was assigned to the left lane (Lane 2). The values of 42 and 51 in. correspond to half of the vehicle widths assuming the dimensions of the design vehicles. The subsequent analysis utilized lateral distance data from right-lane vehicles with reliable speed information, totaling 273,269 vehicles across all 17 locations.

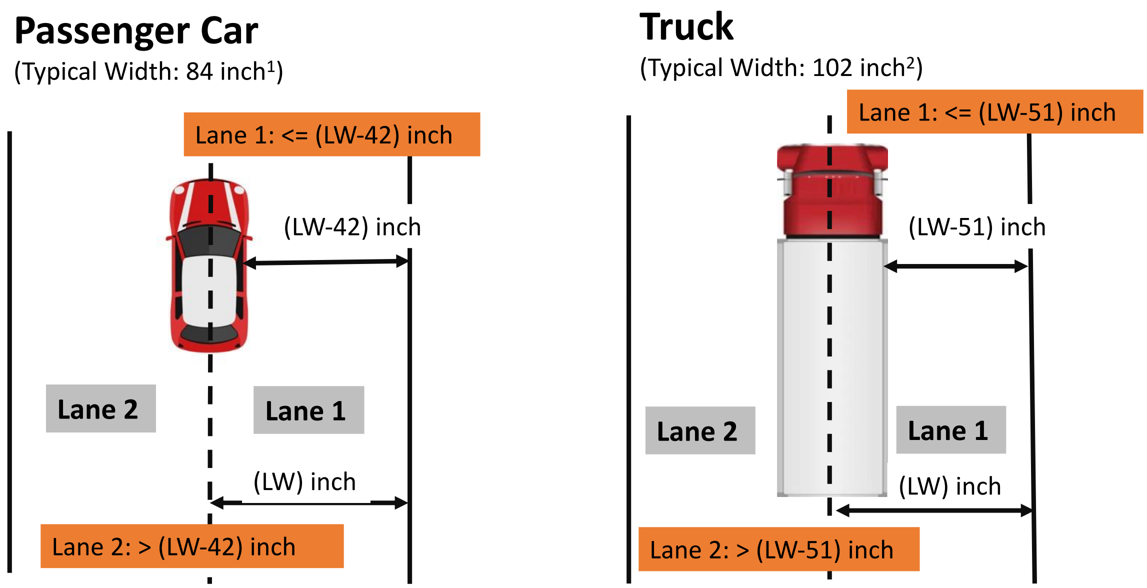

[1]ASHTO 2018, [2]FHWA 2004

Figure 4-1. Lane assignment approach

Sunrise and sunset times for the specific days of data collection were used to assign Day, Night, Dawn, or Dusk to each observation. Observations from sunset to one hour after were assigned Dusk, and observations from one hour before sunrise to sunrise were assigned Dawn. The observations between sunrise and sunset were assigned Day, and the rest were assigned Night. The Dawn and Dusk observations were not included in the comparison between Day and Night.

To illustrate the impact of lane width and shy distance (to the barrier) on vehicles' lateral position, each location was categorized into a bin associated with a specific lane width and shy distance. The 17 locations comprised six unique combinations of lane width and planned right shy distance, as shown in Table 4-1.

Table 4-1. Bins associated with different lane width and right shy distance combinations

Bin	Lane Width (ft)	Right Shy Distance (ft)
11	11	1
12	11	2
21	12	1
22	12	2
23	12	3

4.2. Exploratory Data Analysis

Table 4-2 presents summary statistics of lateral distance to the edge line according to the lane width and shy distance bins. For each location, the speed limit, lane width, planned shy distance to the barrier, and actual shy distance measured at the time of data collection are presented. For lateral distance, the count of vehicles, minimum, maximum, average, standard deviation, and averages during day and night are shown. The vehicle count ranged from 2,000 to over 35,000 thousand. Overall, data from more than a quarter of a million vehicles were used for safety analysis and modeling.

Table 4-2. Summary statistics of lateral distance to edge line by lane width and shy distance bins

Site	Speed Limit (mph)	Lane Width (ft)	Planned Shy Distance (ft)	Measured Shy Distance (in.)	Bin	Count	Lateral Distance (in.)					
							Min	Max	Ave.[1]	Ave. Day	Ave. Night	Std. Dev.[2]
WI-4	60	12	3	33	23	7,061	8.1	100.1	44.0	43.2	46.9	11.0
WI-6	60	12	2	24	22	19,115	4.1	101.7	42.4	41.9	46.1	11.6
WI-7	60	12	2	32	22	13,640	0.2	105.4	42.4	42.0	46.2	10.8
WI-8	60	12	2	34	22	23,647	4.4	103.6	42.0	41.8	44.4	10.7
IL-2	45	12	1	13	21	11,935	12.4	101.7	46.8	45.4	49.8	11.1
IL-3	45	12	1	13	21	19,553	14.3	101.6	51.3	48.6	55.7	11.4
MI-1	60	11	3	30	13	21,667	-10.3	90.0	31.8	31.0	38.4	9.9
WI-2	60	11	2	19	12	5,407	1.2	89.4	41.2	41.2	-	11.4
WI-3	60	11	2	24	12	2,116	1.4	80.2	29.7	29.7	-	9.9
MI-2	60	11	2	22	12	8,636	1.6	89.4	33.1	32.8	37.0	9.5
MI-3	60	11	2	28	12	15,388	0.0	89.5	37.4	36.8	41.0	10.6
MI-4	60	11	2	22	12	21,563	-0.9	89.8	40.1	39.1	47.0	10.2
MI-5	60	11	2	22	12	14,054	-4.8	89	33.3	32.6	36.7	9.3
MI-6	60	11	2	24	12	12,103	-14.1	89.9	33.7	33.4	35.2	9.9
IL-1	45	11	2	24	12	21,989	1.0	90.0	34.3	32.1	37.7	10.2
WI-1	55	11	1	12	11	20,043	20.3	89.9	52.5	50.7	54.6	8.8
WI-5	55	11	1	14	11	35,352	-2.2	90.0	34.2	33.5	39.0	9.7
			All			273,269						

[1] Average; [2] Standard deviation

Readers should note that the actual shy distance to the barrier could differ from the planned shy distance. The actual shy distance was used to compute the distance to the edge line and distance to the barrier. As one might expect, the average lateral distance to the edge line varies between different locations. The underlying pattern in the variation of the lateral distance is examined using probability density plots later in this section. Interestingly, the average lateral distance to the edge line increases during the night compared to during the day at all locations. The differences in the averages range from 1.8 to 7.9 in. This finding is intuitive because drivers tend to veer away from the edge line at night due to visibility constraints. At two of the Mauston locations (WI-2 and WI-3), the right lane was closed during the night. Therefore, the average lateral distance to the edge line was not available for these two locations.

The probability density functions (PDFs) for lateral distance to the edge line at each location are depicted in Figure 4-2. The PDFs of locations with identical lane widths and shy distances are shown in the same color. One can note that the variability within the same-colored plots is less than the variability with the other-colored plots. One exception is the group containing locations WI-1 and WI-5. These were both at the same location: I-43 NB URT under the Overleaf Trail. The difference was that WI-1 was on the older poor-quality pavement, which used the shoulder for the right lane, while WI-5 was on reconstructed/new pavement. The team surmises that the significant difference between these two locations can be attributed to this reason.

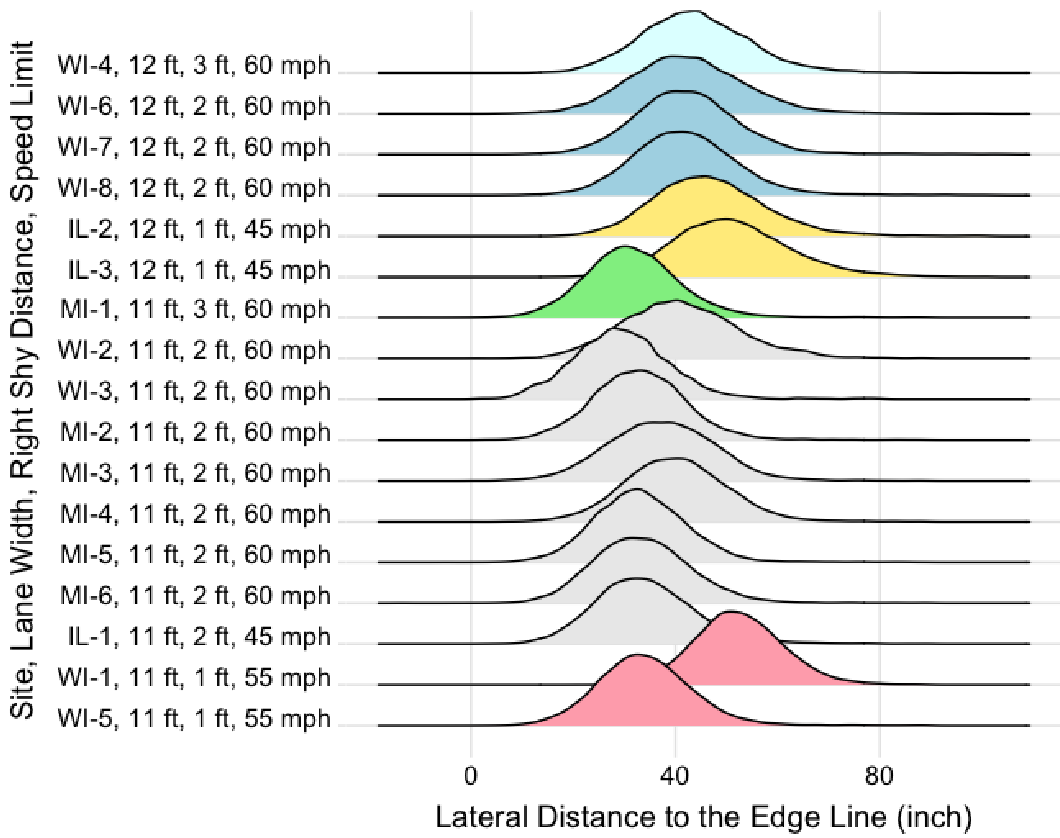

Figure 4-2. Empirical probability density function of lateral distance to the edge line

For a given lane width, as the shoulder width or shy distance to the barrier increases, one can expect drivers to move closer to the edge line. In other words, the lateral distance to the edge line decreases, and this trend is confirmed in Figure 4-2. Readers should note that the amount of decrease in lateral distance to the edge line is smaller than the increase in the shy distance. In other words, while the drivers move closer to the edge line, drivers are farther from the barrier because of the increase in the shy distance. The lateral distance to the barrier is examined next and will illustrate this. For a given shy distance to the barrier, as lane width increases, the lateral distance to the edge line increases. This trend can also be observed in Figure 4-2.

The PDFs for lateral distance to the right barrier at each location are depicted in Figure 4-3. The figure illustrates that the lateral distance to the barrier increases as the lane width or the shy distance to the barrier increases, as one would expect.

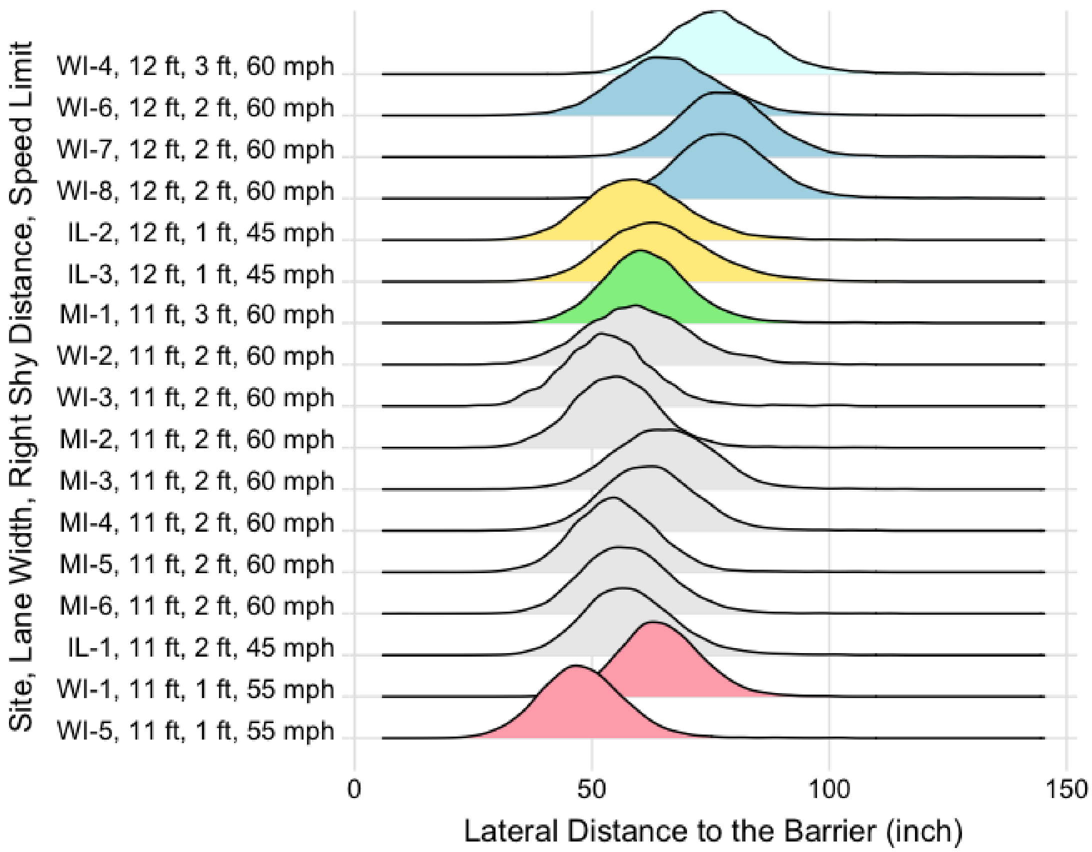

Figure 4-3. Empirical probability density function of lateral distance to the barrier

The exploratory data analysis provides the following intuitive findings:

- The lateral distance to the edge line increases during nighttime compared to daytime.
- The lateral distance to the edge line increases with wider lanes and decreases with wider shy distances.
- The lateral distance to the barrier increases with wider lanes and wider shy distances.

4.3. Analysis and Modeling Methodology

The safety analysis and modeling methodology comprised three components, as shown in Figure 4-4. First, all of the observations, represented by the average lateral distance to the edge line/barrier, were modeled. Next, tail events, represented by the lowest one percentile of the lateral distance observations, were modeled. Finally, the probabilities of edge line encroachment and barrier contact were modeled. All events and tail events were modeled using the standard linear regression approach. The methodology used to model the probabilities of edge line encroachment and barrier contact is described next.

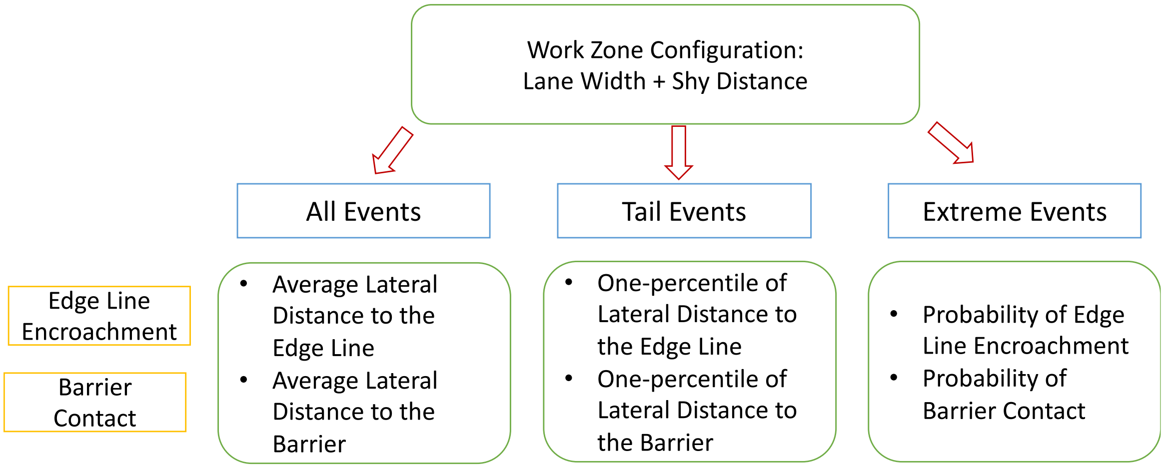

Figure 4-4. Methodology of safety analysis

Extreme value theory (EVT) was used to estimate the likelihood of edge line encroachment and contact with the right-side barrier. EVT estimates crash risk by analyzing all traffic events, bypassing the need for crash data. In this study, the Peak Over Threshold (POT) method with a generalized Pareto (GP) distribution was used for the EVT modeling. The POT method quantifies the stochastic behavior of processes at extreme levels by considering conflicts surpassing specific thresholds. For instance, in Figure 4-5, surrogate safety measures surpassing severity thresholds (S_2) are identified as exceedances or risky events (Tarko 2012). These exceedances are then used for EVT modeling to predict the probability of extreme events (S_3).

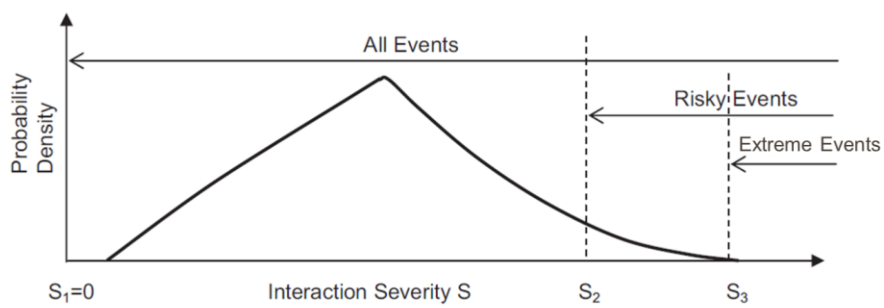

Source: Tarko 2012

Figure 4-5. Illustration of EVT modelling

EVT focuses on the tail of the distribution, with less frequent exceedances occurring as severity increases. The GP distribution, selected for its applicability to tail events surpassing thresholds, was employed to model exceedance distributions. This GP distribution is defined as follows (Tarko 2012):

$$P(S > D_2|x_3) = 1 - F(D_2|x_3) \tag{6}$$

$$f(S|x_3) = \begin{cases} \frac{1}{\sigma} \cdot \left(1 + k \cdot \frac{S-\theta}{\sigma}\right)^{-1-\left(\frac{1}{k}\right)} & for\ (k > 0\ and\ \theta < S)\ or \\ & \left(k < 0\ and\ \theta < S < -\frac{\sigma}{k}\right) \\ \frac{1}{\sigma} \cdot e^{-S-\frac{\theta}{\sigma}} & for\ k = 0\ and\ \theta < S \end{cases} \quad (7)$$

where

S = transformed risk event severity
D_2 = threshold collision proximity
x_3 = exogenous conditions under which the GP distribution is homogeneous
F = cumulative GP distribution
f = GP probability density function
k = shape parameter
σ = scale parameter

Using the statistical tool R, the research team applied the GP distribution with the POT method to model exceedances, providing shape and scale parameters for computing conditional probabilities of extreme events. When modeling lateral distance, the focus was on extreme values, so the negative values of lateral distance to the edge line were utilized in the POT. The optimal threshold (S_2) was identified to ensure statistical reliability and model validity.

Two types of lane departure events were evaluated: edge line encroachment and barrier contact. For edge line encroachment events, where lateral distance is less than zero, S_3 was set to 0. For barrier contact events, where lateral distance is less than the negative of shy distance, S_3 was set to the negative of shy distance. The conditional probability of extreme events given risky events was estimated using the GP distribution. The probability of extreme events was calculated by multiplying the estimated conditional probability by the empirical probability of risky events (the number of exceedances over the number of total observations).

4.4. Modeling of All Events and Tail Events

4.4.1. All Events

The average lateral distances to the edge line and average lateral distances to the barrier represent all events and are shown in Figure 4-6. The plots illustrate that vehicles on wider lanes tend to move farther from the edge line and barrier. Conversely, with greater right shy distances to the barrier, vehicles tend to move closer to the edge line but farther from the barrier.

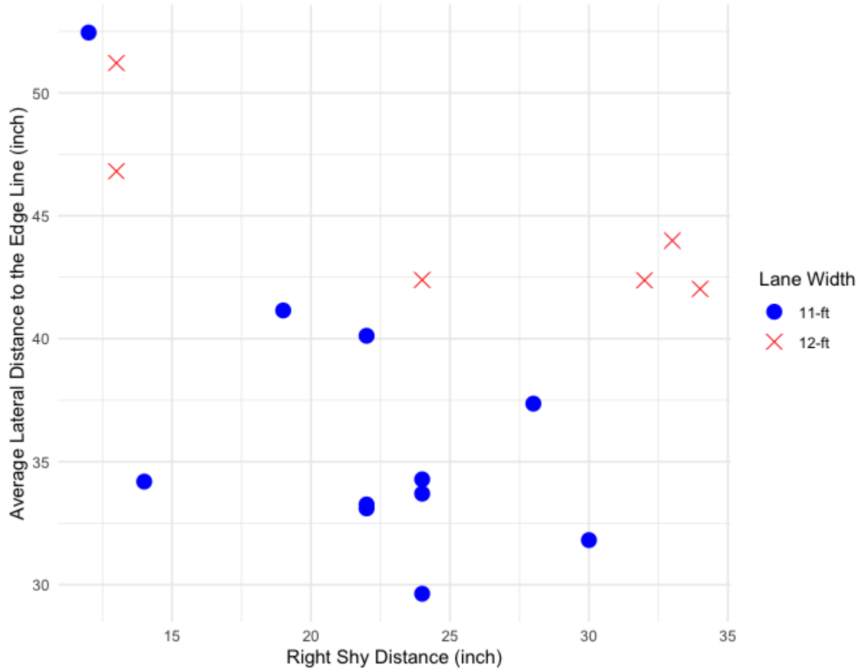

(a) Observed average lateral distance to the edge line

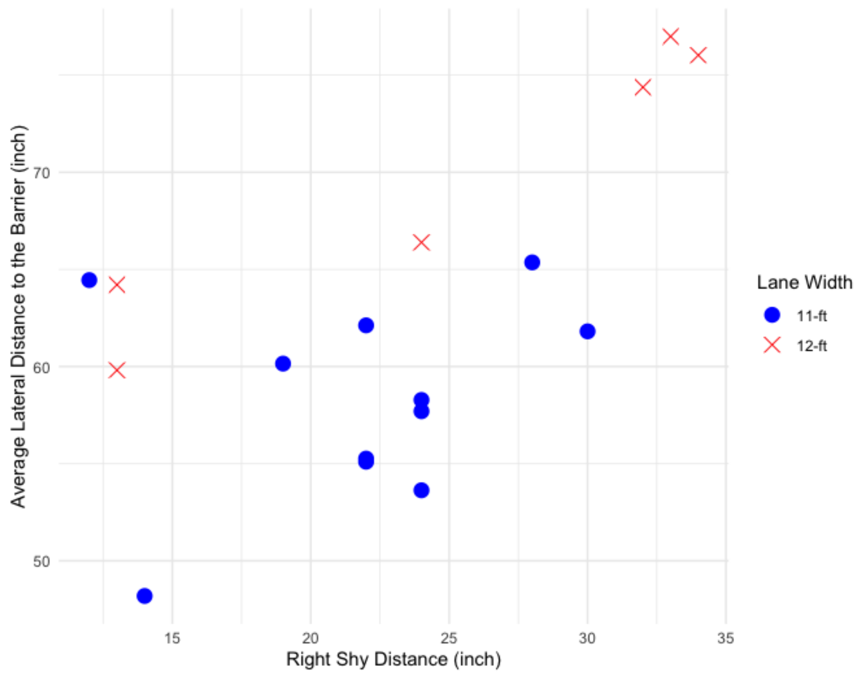

(b) Observed average lateral distance to the barrier

Figure 4-6. Scatter plots of observed average lateral distances

These observations were further validated using linear regression models, as presented in Table 4-3. In these models, lateral distances to the edge line and barrier served as the dependent variables, while lane width and shy distance were independent variables. Both models demonstrate good performance, with lane width and shy distance showing statistical significance (p-value < 0.01).

Table 4-3. Regression analysis of average lane position

Dependent Variable	Average Lateral Distance to Edge Line			
Description	**Coefficient**	**Std. Error**	**t-stat**	**p-value**
Intercept	-60.08	26.63	-2.26	0.04
Lane Width	9.71	2.39	4.06	< 0.01
Shy distance	-0.47	0.17	-2.81	< 0.01
R-square		0.6		
P-value		< 0.001		
Dependent Variable	**Average Lateral Distance to Barrier**			
Description	**Coefficient**	**Std. Error**	**t-stat**	**p-value**
Intercept	-60.08	26.63	-2.26	0.04
Lane Width	9.71	2.39	4.06	< 0.01
Shy distance	0.53	0.17	3.21	< 0.01
R-square		0.71		
P-value		< 0.001		

Figure 4-7 illustrates the effects of lane width and shy distance using the estimates from the regression models. Vehicles on wider lanes (12 ft compared to 11 ft) tend to stay farther away from the edge line and the barrier. Conversely, with greater right shy distances to the barrier (36 in. compared to 24 in. and 12 in.), vehicles tend to move closer to the edge line but farther from the barrier.

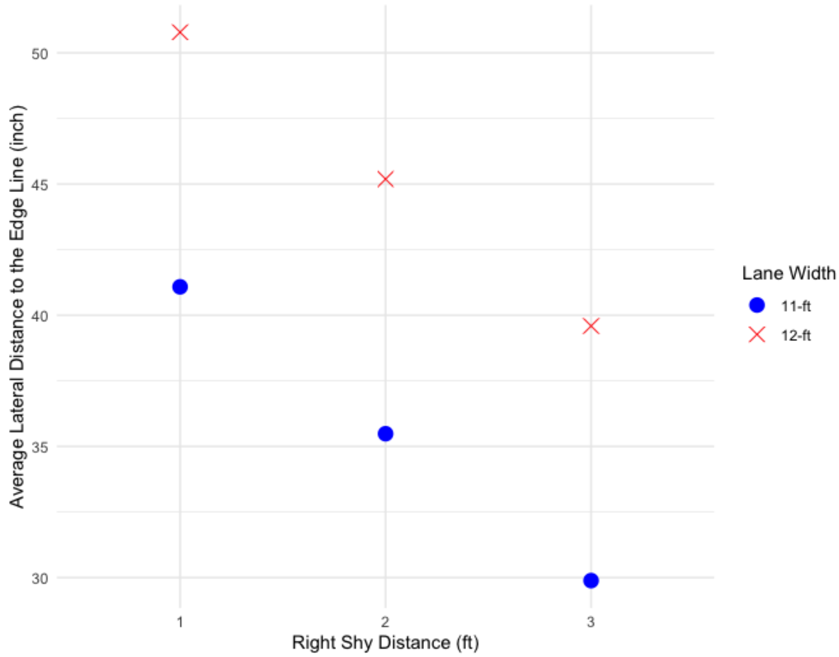

(a) Average lateral distance to edge line

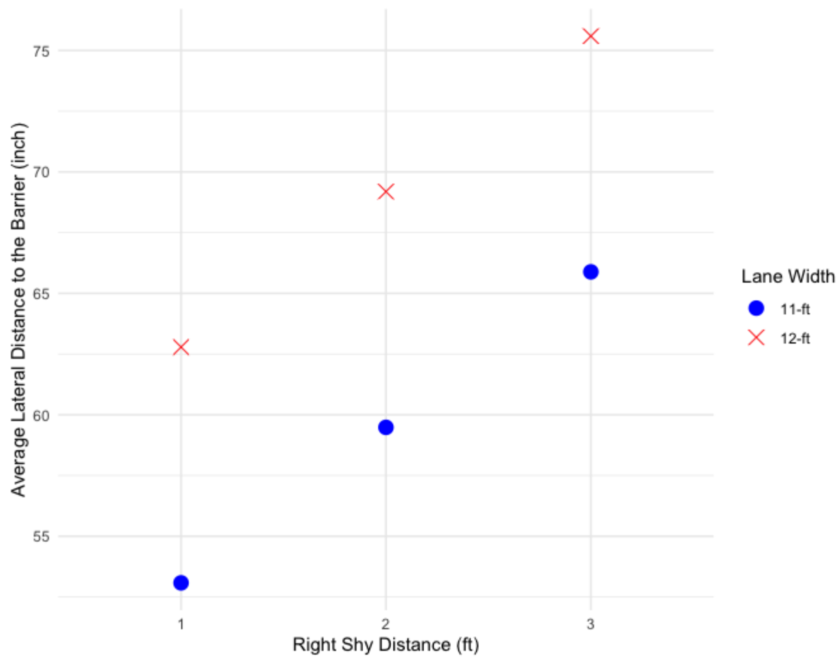

(b) Average lateral distance to barrier

Figure 4-7. Impact of lane width and shy distance on average lateral distances

4.4.2. Tail Events

Tail events are represented by the lowest one percentile of the lateral distance observations. Tail events are similar to the risky events shown in Figure 4-5, which have a high chance to become extreme events (edge line encroachment or barrier contact). The one-percentile lateral distance to the edge line and one-percentile lateral distance to the barrier for different work zone configurations are plotted in Figure 4-8. The plots indicate that the one-percentile vehicles on wider lanes tend to move farther from the edge line and the barrier. The one-percentile vehicles on wider shoulders tend to move closer to the edge line but farther from the barrier.

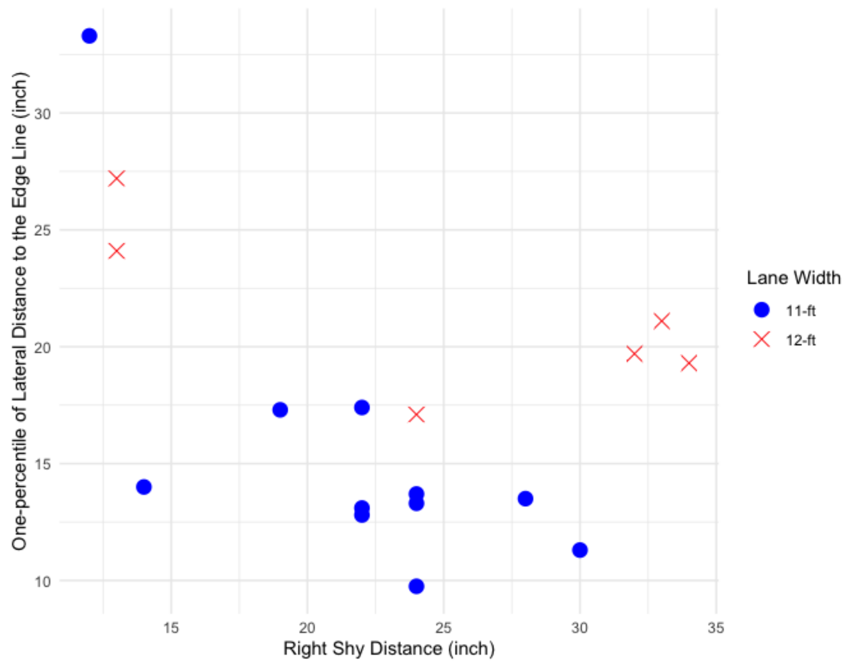

(a) One-percentile lateral distance to the edge line

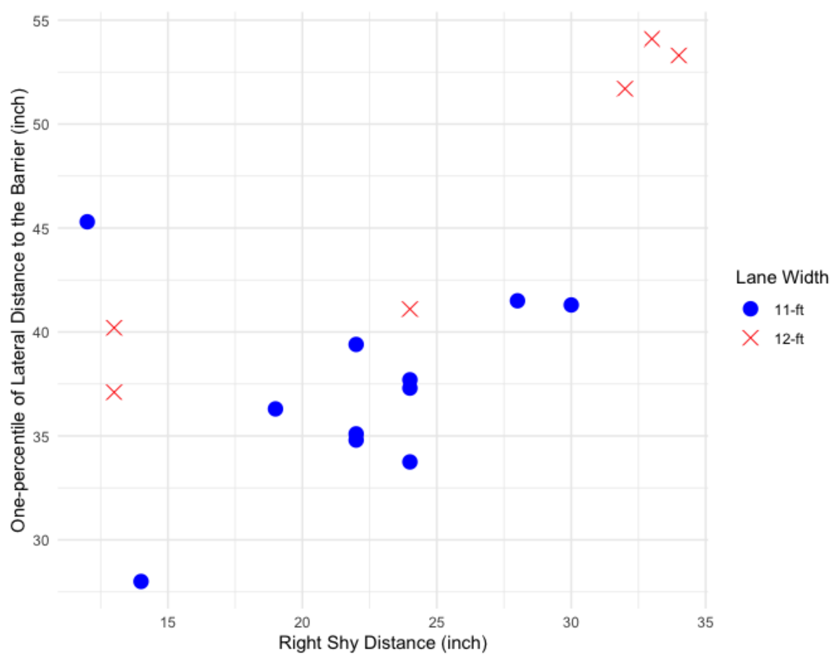

(b) One-percentile lateral distance to the barrier

Figure 4-8. Scatter plots of observed one-percentile lateral distances

These observations were corroborated using linear regression models, as depicted in Table 4-4. Both models demonstrate good performance, with lane width and shy distance showing statistical significance (p-value < 0.01).

Table 4-4. Regression analysis of tail lane position

Dependent Variable	**One Percentile of Lateral Distance to Edge line**			
Description	**Coefficients**	**Std. Error**	**t-stat**	**p-value**
Intercept	-55.64	26.42	-2.11	0.05
Lane Width	7.41	2.37	3.13	<0.01
Shy distance	-0.48	0.16	-2.9	<0.01
R-square		0.52		
P-value		<0.010		
Dependent Variable	**One Percentile of Lateral Distance to Barrier**			
Description	**Coefficients**	**Std. Error**	**t-stat**	**p-value**
Intercept	-55.64	26.42	-2.11	0.05
Lane Width	7.41	2.37	3.13	<0.01
Shy distance	0.52	0.16	3.16	<0.01
R-square		0.64		
P-value		< 0.001		

Figure 4-9 shows the effects of lane width and shy distance using the regression models for tail events. Specifically, the one-percentile vehicles on wider lanes (12 ft compared to 11 ft) tend to move farther from the edge line and the barrier. The one-percentile vehicles with wider shy distances (3 ft compared to 2 ft and 1 ft) tend to gravitate closer to the edge line but farther from the barrier.

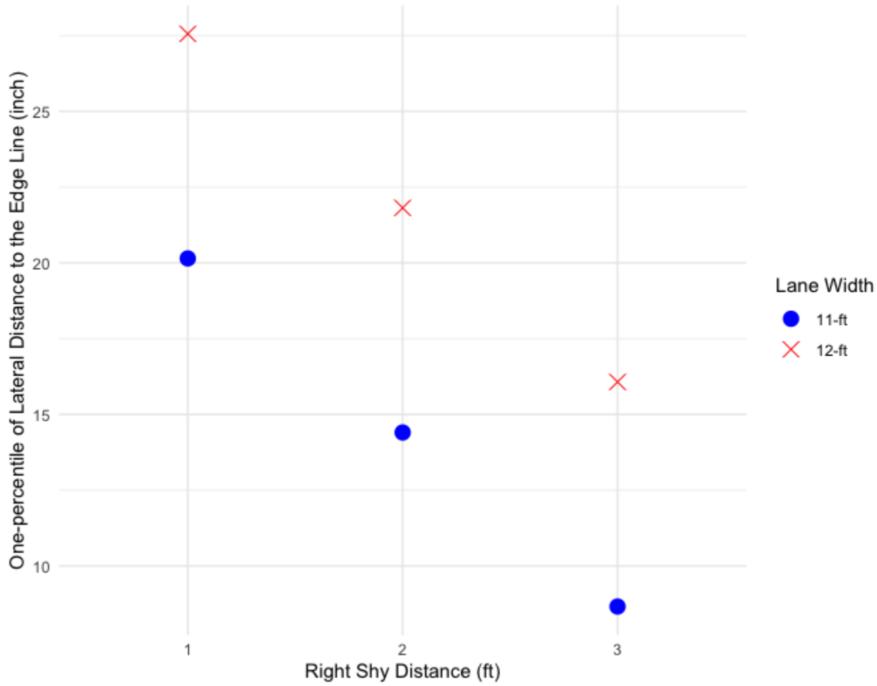

(a) One-percentile lateral distance to the edge line

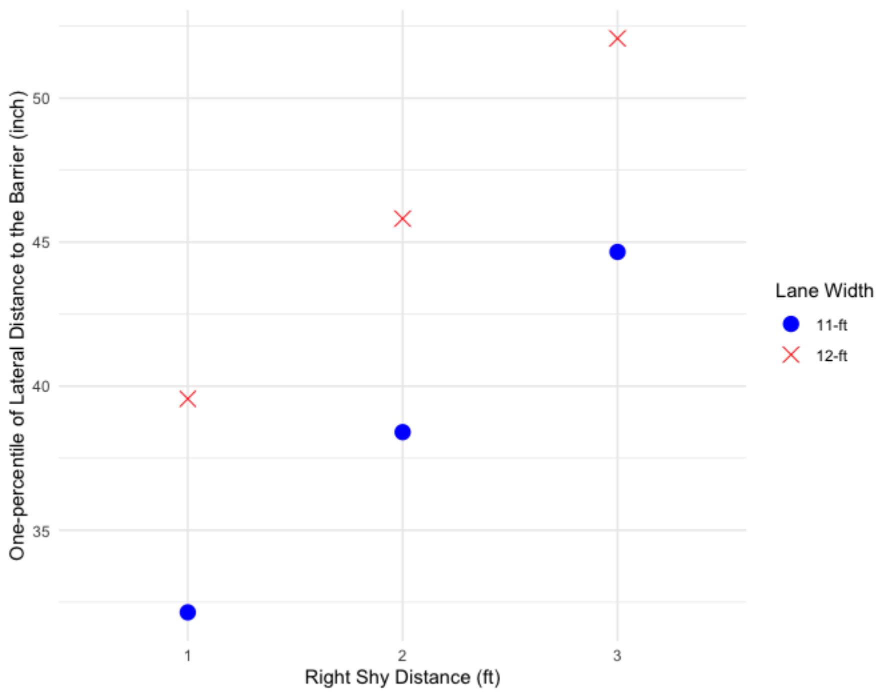

(b) One-percentile lateral distance to the barrier

Figure 4-9. Impact of lane width and shy distance on risky events

4.5. Probability of Edge Line/Barrier Encroachment

The research team developed a comprehensive EVT model utilizing data from all sites to capture the impact of all of the variables of interest. This approach provided more exceedances than when EVT models were developed for individual locations. The full model is nonstationary and incorporates covariates in the scale parameter estimation. The shape parameter remains unchanged due to the absence of factual evidence indicating nonstationarity in tail behavior; thus, no covariates were included in its estimation (Coles et al. 2001).

The covariates included were lane width, shy distance, road curvature, and speed limit, along with vehicle-level variables including time of day (day or night), free flow conditions, vehicle type (passenger car or truck), and adjacency to other vehicles. Various combinations of these variables were assessed using the likelihood ratio test to streamline model structures and variable inclusions. The nonstationary model, which incorporates a linear combination of lane width and shy distance in the scale parameter, exhibits significance, with a small p-value of 0.02 in a likelihood ratio test compared to the stationary model. However, when additional terms such as the interaction between lane width and shy distance or other covariates such as time of day are included in the linear combination, the model loses significance, as indicated by a larger p-value exceeding 0.1 in a likelihood ratio test compared to the previous nonstationary model.

Consequently, the final model incorporates a linear combination of lane width and shy distance in the scale parameter. The optimal threshold of 12 in. results in 1,147 exceedances (out of a total of 273,269 vehicles), which were used to develop the EVT model. As depicted in Table 4-5, estimation results of the final model reveal a negative scale parameter for lane width, signifying that an increase in lane width reduces the scale parameter and, consequently, the variance of the lateral distance distribution. This reduction indicates a decrease in the probability of extreme events. Conversely, a positive scale parameter for shy distance indicates that an increase in shy distance augments the scale parameter and hence the variance of the lateral distance distribution. This increase suggests a rise in the probability of extreme events.

Table 4-5. Estimation results for the POT model

Description	Estimated Value	Standard Error	P-value
Shape Parameter, k	0.01	0.03	
Scale Parameter, σ_0	7.59	2.92	<0.01
Scale Parameter, $\sigma_1$lane width)	-0.51	0.27	0.06
Scale Parameter, σ_2 (shy distance)	0.04	0.01	<0.01
Negative Loglikelihood	2,354.117		
Number of Observations	273,269		
Threshold (inches)	12		
Number of Exceedances/risky Events	1,147		

Figure 4-10 illustrates the impact of lane width and shy distance on the probability of edge line encroachment and barrier contact. An increase in lane width leads to a reduction in the probability of edge line encroachment and barrier contact. An increase in shy distance results in an increase in the probability of edge line encroachment and a decrease in the probability of barrier contact. For an 11 ft lane, the probability of barrier contact approaches zero for a 3 ft right shy distance. Similarly, for a 12 ft lane, the probability of barrier contact approaches zero for a 2 ft shy distance.

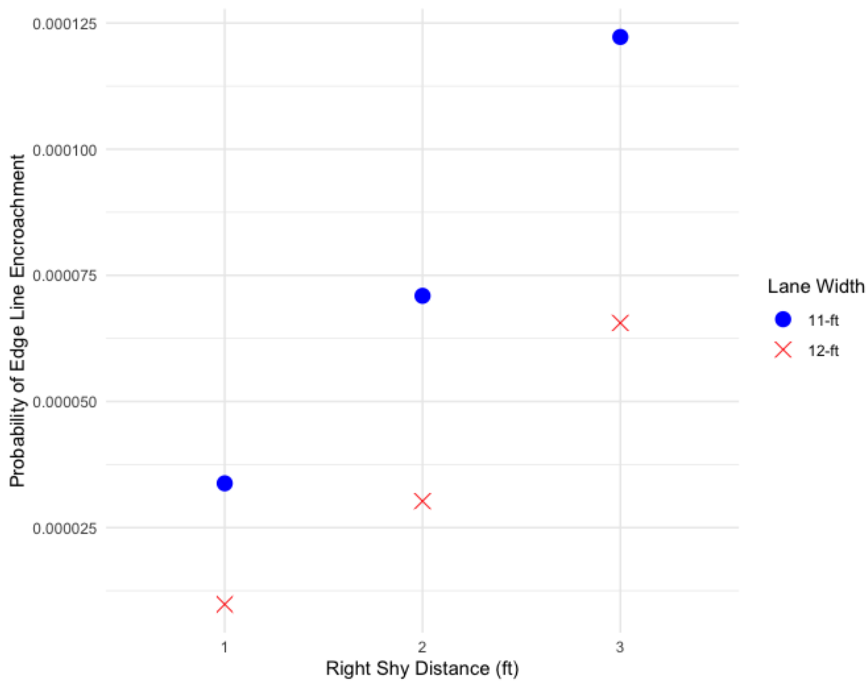

(a) Probability of edge line encroachment

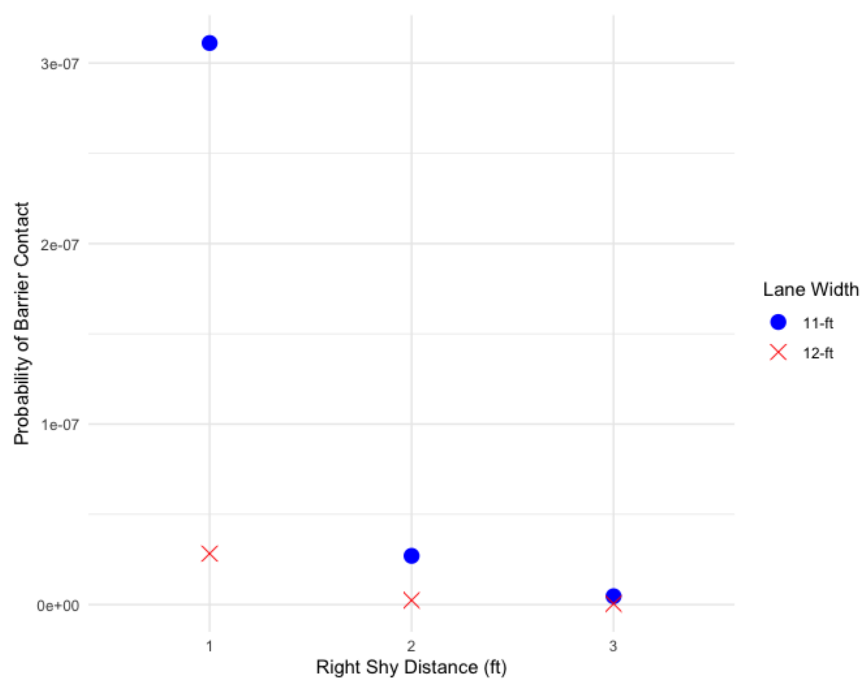

(b) Probability of barrier contact

Figure 4-10. Impact of lane width and shy distance on extreme events

4.6. Summary of Safety Analysis

Vehicles' lateral position in the right travel lane was used as a surrogate safety measure to understand the safety impact of lane width and shy distance. Lateral distance data of over a quarter of a million vehicles collected at 17 locations in three states were used for the safety analysis. All 17 locations had two lanes open in the work zone. The lane widths were either 11 or 12 ft, and the right shy distances were 1, 2, or 3 ft. The safety analysis only considered right departures for vehicles in the right lane. Left departures of vehicles in the right lane or left-lane vehicle encroachments were not modeled because the data collection device could only be installed on the right barrier.

An exploratory data analysis of the average lateral distances to the edge line and barrier was conducted. Lateral distance to the edge line and barrier increased during nighttime compared to daytime. In other words, compared to the daytime, vehicles moved farther away from the edge line and barrier in the nighttime. Lateral distance to the edge line increased with wider lanes and decreased with wider shy distances. Lateral distance to the barrier increased with wider lanes and wider shy distances.

Modeling of all events and tail events was accomplished by linear regression of the average lateral distance of all vehicles and the one-percentile lateral distance, respectively. Lane width and shy distance significantly influenced vehicles' lateral position in relation to the edge line and barrier. All vehicles and tail vehicles tended to move farther from the edge line and the barrier in 12 ft lanes compared to 11 ft lanes. All vehicles and tail vehicles tended to gravitate closer to the edge line but farther from the barrier with larger shy distances (3 ft compared to 2 ft and 1 ft).

EVT modeling was conducted to estimate the probabilities of right edge line encroachment and right barrier contact. Narrower lanes were found to contribute to increased edge line encroachment and barrier contact, while wider shy distances were associated with increased edge line encroachment and reduced barrier contact. Both of these findings are intuitive. The EVT models can be used to estimate the right edge line encroachment and right barrier contact probabilities (for vehicles in the right lane) for different combinations of lane width and shy distance.

As mentioned earlier, the safety analysis only considered right departures of vehicles in the right lane. Only four locations had a 1 ft shy distance, and all of these were very short sections (a few hundred feet), and that could have impacted the findings. This research demonstrates how lateral distance data can be collected and analyzed to model safety. Future research efforts should capture lateral distance from both sides and estimate lane departures in both directions and for vehicles in both lanes.

5. MOBILITY ANALYSIS

Mobility analysis in this project focused on free flow speed given its vital role in estimating other mobility impacts such as capacity and queue length. This chapter describes data processing, an exploratory data analysis, the analysis and modeling methodology used, and finally the estimation of free flow speed.

5.1. Data Processing

Free flow vehicles have been defined in the literature as vehicles with headways greater than or equal to four seconds (Chitturi and Benekohal 2005). Therefore, that threshold was used to identify free flow vehicles. As mentioned in Section 3.2, speed estimation was challenging, and vehicles with reliable speed estimates were flagged. The speed analysis was limited to free flow vehicles with reliable speed estimates. A standard outlier analysis was performed to remove the outliers before performing any other analysis.

$$Lower\ Bound = Q_1 - 1.5 \cdot IQR \tag{8}$$

$$Upper\ Bound = Q_3 + 1.5 \cdot IQR \tag{9}$$

The interquartile range (IQR) is a measure to evaluate statistical dispersion and identify outliers in the sample data. The median is the 50th percentile (Q_2). The interquartile range is equal to the difference between the 75th percentile (Q_3) and 25th percentile (Q_1). To identify outliers, lower and upper limits are calculated using the interquartile range. Observations beyond the two bounds were considered outliers and were removed from the analysis.

5.2. Exploratory Data Analysis

A summary of the number of observations and descriptive statistics for speed at each location are provided in Table 5-1. Overall, speed data from 125,447 free flow vehicles were used, and the number of free flow vehicles at each location ranged from 2,000 to 15,000. Free flow vehicles in both lanes were included in the analysis. Eleven sites had 11 ft lanes and six sites had 12 ft lanes. Left and right shy distances to the barriers ranged from 1 to 3 ft. Ten sites had the same left and right shy distances, while four sites had different left and right shy distances. Three sites in Illinois had a posted speed limit of 45 mph, two sites in Wisconsin had a posted speed limit of 55 mph, and the rest of the sites had a posted speed limit of 60 mph. The average speeds ranged between 54 and 70 mph, which were highly associated with the posted speed limit. The difference between the average speed and speed limit ranged from -0.8 to 14.1 mph, which indicates that the average speed was as high as 14.1 mph over the speed limit (IL-2) or 0.8 mph under the speed limit (WI-1). WI-1 had 11 ft lanes with 1 ft shy distances, had poor pavement, used the shoulder as the right lane, and was immediately upstream of an exit ramp. These factors probably contributed to the free flow speed being lower than the speed limit at this location.

Table 5-1. Summary of speed data

Site	Lane Width (ft)	Planned Shy Dist.[1] (ft)		Speed Limit (mph)	Speed (mph)					Speed Diff.[4] (mph)
		Left	Right		Count	Min	Max	Ave.[2]	St. Dev.[3]	
WI-4	12	2	3	60	4,423	44.1	77.8	61.2	6.0	1.2
WI-6	12	2	2	60	10,007	51.5	78.8	65.5	5.2	5.5
WI-7	12	2	2	60	6,648	46.3	75.6	61.1	5.2	1.1
WI-8	12	2	2	60	14,988	54.0	85.0	69.5	5.8	9.5
IL-2	12	3	1	45	7,063	40.5	77.8	59.1	6.8	14.1
IL-3	12	3	1	45	13,673	38.0	72.6	55.7	6.4	10.7
MI-1	11	2	3	60	9,127	46.3	87.7	67.3	7.6	7.3
WI-2	11	2	2	60	4,692	41.4	83.6	63.1	8.2	3.1
WI-3	11	2	2	60	3,007	42.8	87.7	66.1	8.9	6.1
MI-2	11	2	2	60	2,327	47.5	87.7	71.0	7.8	11.0
MI-3	11	2	2	60	4,638	42.8	87.7	67.2	8.5	7.2
MI-4	11	2	2	60	7,451	44.5	87.7	66.5	7.9	6.5
MI-5	11	2	2	60	3,170	50.7	87.7	69.9	7.0	9.9
MI-6	11	2	2	60	7,482	46.7	87.7	69.0	8.1	9.0
IL-1	11	2	2	45	12,502	31.4	82.4	57.1	9.3	12.1
WI-1	11	1	1	55	6,121	38.3	69.9	54.2	5.8	-0.8
WI-5	11	1	1	55	8,128	38.8	71.6	55.1	6.1	0.1
		All			125,447					

[1] Distance to barrier; [2] Average speed; [3] Standard deviation; [4] Speed difference = average speed - speed limit

The PDFs for free flow speed at each location are depicted in Figure 5-1. The PDFs of locations with identical lane widths and shy distances are shown in the same color.

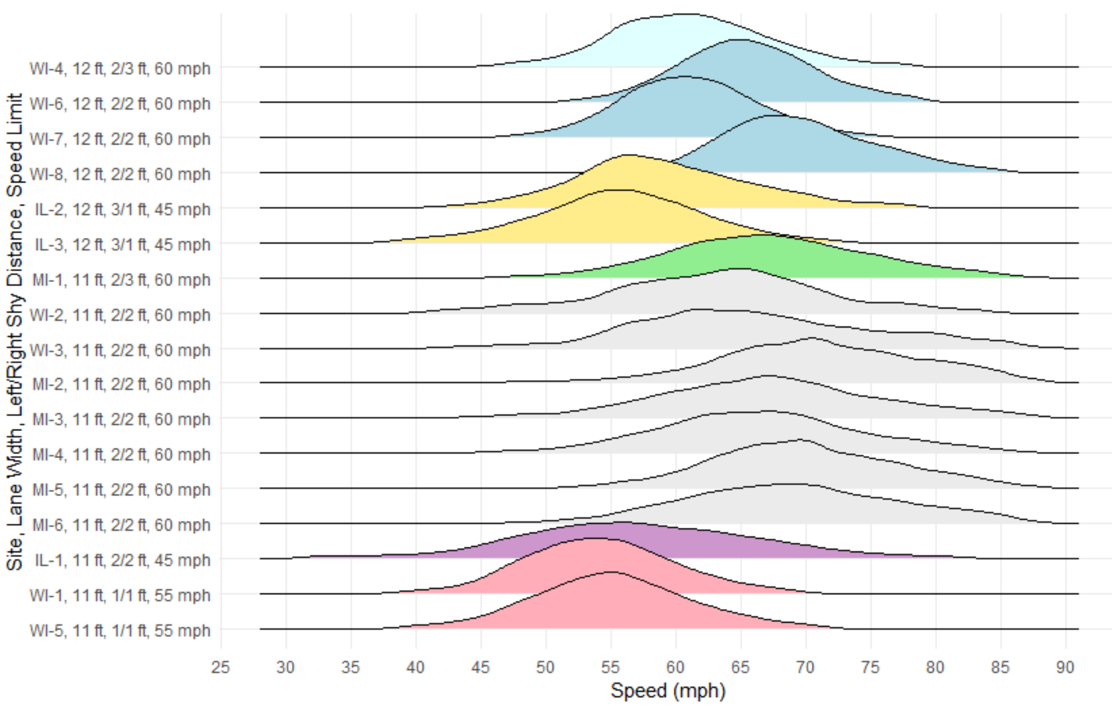

Figure 5-1. Empirical probability density function of free flow speed by location

One can notice that the variability within the same-colored plots is less than the variability with the other-colored plots. The one exception is the group containing locations WI-6, WI-7, and WI-8. WI-7 had lower free flow speeds than the other two locations although they share the same geometry. WI-7 was about a quarter of a mile downstream of an entrance ramp, and that could have contributed to the lower free flow speeds at this location.

Free flow speed variation by lane was evaluated using paired t-tests. Statistical tests such as the t-test are used to compare the means of two distributions and assess whether there is a statistically significant difference between the mean estimates. The t-test consists of the hypothesis, difference of mean values, variance of each group, number of observations in each group, t-statistic, and critical value. In this study, two sample t-tests were implemented with the following hypotheses:

$$H_o: \mu_1 - \mu_2 = 0 \tag{10}$$

$$H_a: \mu_1 - \mu_2 \neq 0 \tag{11}$$

$$t\ stat = \frac{\mu_1 - \mu_2}{\frac{(n_1-1)\times{\sigma_1}^2 + (n_2-1)\times{\sigma_2}^2}{n_1+n_2+2} \cdot \sqrt{\frac{1}{n_1}+\frac{1}{n_2}}} \tag{12}$$

where

μ_1, μ_2 = mean values of each sample set
σ_1, σ_2 = variance of each of sample set
n_1, n_2 = number of observations in each sample set
$t\ stat$ = t-statistic

The t-statistic is compared against the critical value from the t-distribution. Higher values of the t-statistic indicate a large difference between the two sample sets. The smaller the t-statistic, the more similar the two sample sets are.

The results for the lane-level analysis are provided in Table 5-2. The difference in speed was calculated as the average speed in the right lane minus the average speed in the left lane. Therefore, negative values indicate that the left lane had higher speeds than the right lane. While 14 locations (out of 17) had numerically higher speeds in the left lane, the difference was statistically significant at 12 locations. At 3 locations, the average speed in the right lane was greater than the average speed in the left lane, with the differences being 0.4 mph, 0.6 mph, and 1.6 mph. The research team could not correlate this behavior to pavement condition, uneven lanes, or any other known factors.

Table 5-2. Summary of speed data and statistical tests by travel lane

Site	Cat.[1]	Cond.[2]	Speed (mph) Obs.[3]	Ave.[4]	St. Dev.[5]	Student's t-Test Diff.[6]	t-stat	p-value
WI-1	Lane	R	4,010	53.9	5.8	-0.8	-5.1	< 0.001
		L	2,111	54.7	5.7			
WI-2	Lane	R	2,425	63.9	6.0	1.6	6.7	< 0.001
		L	2,267	62.3	10.0			
WI-3	Lane	R	1,303	63.2	6.1	-5.1	-16.2	< 0.001
		L	1,704	68.3	9.9			
WI-4	Lane	R	4,045	60.7	5.7	-6.3	-20.4	< 0.001
		L	378	67.0	6.5			
WI-5	Lane	R	5,192	55.4	6.0	0.6	4.2	< 0.001
		L	2,936	54.8	6.2			
WI-6	Lane	R	7,548	64.9	5.1	-2.6	-21.6	< 0.001
		L	2,459	67.4	5.0			
WI-7	Lane	R	5,981	61.1	5.1	-0.3	-1.4	0.158
		L	667	61.4	6.1			
WI-8	Lane	R	9,958	68.0	5.3	-4.7	-51.0	< 0.001
		L	5,030	72.6	5.4			
MI-1	Lane	R	5,558	67.2	7.4	-0.4	-2.1	0.032
		L	3,569	67.5	7.9			
MI-2	Lane	R	1,968	70.8	7.5	-1.0	-2.3	0.020
		L	359	71.9	9.2			
MI-3	Lane	R	3,847	67.1	7.8	-0.8	-2.5	0.012
		L	791	67.9	11.2			
MI-4	Lane	R	5,021	66.2	7.3	-1.0	-5.0	< 0.001
		L	2,430	67.2	8.9			
MI-5	Lane	R	3,105	69.9	7.0	-0.6	-0.7	0.485
		L	65	70.5	7.9			
MI-6	Lane	R	5,476	67.4	7.5	-5.7	-28.4	< 0.001
		L	2,006	73.1	8.2			
IL-1	Lane	R	7,377	53.9	7.7	-7.7	-50.3	< 0.001
		L	5,125	61.7	9.5			
IL-2	Lane	R	5,422	58.2	6.5	-3.7	-19.7	< 0.001
		L	1,641	61.9	7.1			
IL-3	Lane	R	8,708	55.8	6.4	0.4	3.6	< 0.001
		L	4,965	55.4	6.5			

[1] Category; [2] Condition: L is left lane and R is right lane; [3] Number of observations; [4] Average; [5] Standard deviation; [6] Difference equals average speed of right lane minus average speed of left lane

Given that data were collected for up to two days at each location, speed data were available by time of day. Therefore, free flow speeds at night were compared to free flow speeds during the day, and the results are presented in Table 5-3. The difference in speed was calculated as the average speed during daytime minus the average speed during nighttime, so negative values indicate that nighttime speeds were greater than daytime speeds. Eleven out of 17 sites showed statistically significant higher speeds during nighttime compared to daytime. This is different from the *Highway Capacity Manual*, which indicates that free flow speeds are greater during the day (TRB 2022). Wisconsin locations WI-1 and WI-5 had lighting, and this could possibly explain the higher speeds during nighttime. However, a similar correlation between lighting and higher speeds at night could not be found for the Illinois and Michigan locations.

Table 5-3. Summary of speed data and statistical tests by day and night

			Speed (mph)			Student's t-Test		
Site	**Cat.**[1]	**Cond.**[2]	**Obs.**[3]	**Ave.**[4]	**St. Dev.**[5]	**Diff.**[6]	**t-stat**	**p-value**
WI-1	Time	Day	1,710	52.0	5.5	-3.2	-20.5	< 0.001
		Night	3,860	55.2	5.4			
WI-2	Time	Day	3,546	64.0	7.9	4.2	14.0	< 0.001
		Night	908	59.9	8.7			
WI-3	Time	Day	1,997	66.0	8.4	-0.1	-0.2	0.828
		Night	789	66.1	9.6			
WI-4	Time	Day	3,155	61.4	6.0	1.0	4.3	< 0.001
		Night	921	60.5	6.1			
WI-5	Time	Day	4,995	54.4	6.2	-1.5	-9.6	< 0.001
		Night	2,129	55.9	5.7			
WI-6	Time	Day	7,787	65.7	5.2	1.4	9.3	< 0.001
		Night	1,475	64.4	5.2			
WI-7	Time	Day	5,205	61.2	5.2	0.8	4.2	< 0.001
		Night	876	60.4	5.3			
WI-8	Time	Day	12,073	69.7	5.7	1.2	8.4	< 0.001
		Night	1,769	68.4	5.7			
MI-1	Time	Day	6,403	66.1	7.6	-4.1	-20.1	< 0.001
		Night	1,703	70.2	7.0			
MI-2	Time	Day	1,873	70.6	7.6	-2.4	-4.9	< 0.001
		Night	274	73.0	8.5			
MI-3	Time	Day	3,117	65.6	8.5	-5.1	-17.1	< 0.001
		Night	1,015	70.7	7.7			
MI-4	Time	Day	4,765	65.3	7.7	-2.9	-13.2	< 0.001
		Night	1,762	68.2	7.9			
MI-5	Time	Day	1,767	69.0	7.0	-2.2	-7.8	< 0.001
		Night	943	71.2	7.0			
MI-6	Time	Day	5,663	67.9	7.9	-4.1	-16.1	< 0.001
		Night	1,131	72.0	7.9			
IL-1	Time	Day	5,048	55.0	10.0	-4.0	-22.9	< 0.001
		Night	6,105	59.0	8.5			
IL-2	Time	Day	3,527	58.4	6.6	-1.6	-9.5	< 0.001
		Night	2,851	60.0	6.9			
IL-3	Time	Day	6,645	54.2	6.4	-3.9	-35.8	< 0.001
		Night	5,559	58.1	5.5			

[1] Category; [2] Condition; [3] Number of observations; [4] Average; [5] Standard deviation; [6] Difference equals average speed during daytime minus average speed during nighttime; positive values indicate daytime speed is greater than nighttime speed, and negative values indicate nighttime speed is greater that daytime speed.

5.3. Analysis and Modeling Methodology

Linear regression was used in this research to model free flow speeds. The *Highway Capacity Manual* uses the same approach to relate free flow speed to variables of interest (TRB 2022).

Linear regression is a statistical modeling approach that establishes linear relationships between response and exploratory variables. The least squares approach was implemented to fit the model to the observed data. The method consists of minimizing the sum of the squares of vertical deviations in each data point. Model coefficients contribute to evaluate the effects of predictor variables. Linear regression has the following model form:

$$y_i = \beta_0 + \beta_1 \cdot x_{i1} + \cdots + \beta_m \cdot x_{im} + \varepsilon_i \qquad i = 1, \ldots, n \tag{13}$$

A correlation analysis was implemented to evaluate the statistical relationships among the variables considered for modeling speed. Through regression modeling, linear regression models were developed with speed as the dependent variable and geometric and operational measures as the independent variables. Measures of goodness of fit included the statistical significance of model coefficients, confidence intervals, and R^2.

5.4. Free Flow Speed Estimation

Using speed data, linear regression was implemented to develop models to predict free flow speeds in work zones with various geometric and operational variables. In preparation for modeling, data distribution and availability were reviewed for every predictor variable. Table 5-4 shows the number of vehicles and percentage of total vehicles by lane for the 17 locations. Five locations—WI-4, WI-7, MI-2, MI-3, and MI-5—had a small number of reliable speed observations in the left lane. Data from the left lane were only available for 2% to 17% of the overall observations at those locations. Therefore, the decision was made to exclude those locations from modeling because the observations from the right lane would have been overrepresented, which could have introduced bias into the model estimates. As a result, the 12 locations where at least 25% of the observations were in the left lane were included in the model. A total of 94,200 observations were used for the regression modeling.

Table 5-4. Number and percentage of observations by travel lane

	Lane Position				
	1		2		All
Site	Obs.	%	Obs.	%	Obs.
WI-1	4,010	66%	2,111	34%	6,121
WI-2	2,425	52%	2,267	48%	4,692
WI-3	1,303	43%	1,704	57%	3,007
WI-4	4,045	91%	378	9%	4,423
WI-5	5,192	64%	2,936	36%	8,128
WI-6	7,548	75%	2,459	25%	10,007
WI-7	5,981	90%	667	10%	6,648
WI-8	9,958	66%	5,030	34%	14,988
MI-1	5,558	61%	3,569	39%	9,127
MI-2	1,968	85%	359	15%	2,327
MI-3	3,847	83%	791	17%	4,638
MI-4	5,021	67%	2,430	33%	7,451
MI-5	3,105	98%	65	2%	3,170
MI-6	5,476	73%	2,006	27%	7,482
IL-1	7,377	59%	5,125	41%	12,502
IL-2	5,422	77%	1,641	23%	7,063
IL-3	8,708	64%	4,965	36%	13,673
All	**86,944**	**69%**	**38,503**	**31%**	**125,447**

For regression modeling, variables were considered as continuous variables or were designated as ordinal indicators. The variables had the following coding and units:

SP = free flow speed (mph)
SL = posted speed limit (mph)
LN = lane position (0=lane 1, 1=lane 2)
LNW = lane width (ft)
$RSHD$ = right shy distance to barrier (ft)
$LSHD$ = left shy distance to barrier (ft)
DN = time of the day (0=day, 1=night)
VEH = vehicle type (0=passenger, 1=truck)
$FEED$ = speed feedback sign (0=not present, 1=present)
LOC = site location (0=Wisconsin, 1=Michigan, 2=Illinois)

In the modeling process, correlations among the variables were evaluated to determine the strength of the relationships among the variables. The results of the correlation analysis are provided in Table 5-5. Work zone speeds (SP) were found to have a correlation coefficient of 0.49 with speed limit (SL) and 0.45 with right shy distance (RSHD). The significant correlation with speed limit is expected. Speed limit (SL) has correlation factors within ±0.5 with other predictor variables such as LN, RSHD, LSHD, DN, and VEH.

Table 5-5. Correlation coefficients

Variable	SP	SL	LN	LNW	$RSHD$	$LSHD$	DN	VEH	$FEED$
SP	1.00								
SL	0.49	1.00							
LN	0.12	-0.01	1.00						
LNW	0.08	-0.17	-0.07	1.00					
$RSHD$	0.45	0.57	0.03	-0.30	1.00				
$LSHD$	0.00	-0.51	-0.03	0.60	-0.14	1.00			
DN	-0.10	-0.29	-0.02	-0.08	-0.20	0.02	1.00		
VEH	-0.17	-0.21	0.02	0.03	-0.07	0.22	0.04	1.00	
$FEED$	0.02	0.18	0.05	-0.20	0.09	-0.02	-0.05	0.15	1.00

Based on the data available and intended application, two models were developed. Model 1 is more disaggregate and quantifies the effects of the geometric and operational variables, including travel lane and vehicle type. Model 2 uses the same predictors as Model 1 except vehicle type and travel lane. The idea is that Model 2 can be used by work zone designers to estimate free flow speed in work zones at the design stage. Models 1 and 2 are provided in Equations 14 and 15.

$$SP = 0.80 \cdot SL + 2.61 \cdot LN + 2.60 \cdot LNW + 3.27 \cdot RSHD$$
$$+2.98 \cdot LSHD + 1.98 \cdot DN - 1.83 \cdot VEH - 1.36 \cdot FEED + 1.24 \cdot LOC - 25.18 \quad (14)$$

$$SP = 0.85 \cdot SL + 2.95 \cdot LNW + 3.26 \cdot RSHD + 2.21 \cdot LSHD$$
$$+1.90 \cdot DN - 1.43 \cdot FEED + 1.66 \cdot LOC - 29.93 \quad (15)$$

Table 5-6 includes the model coefficients and measures of goodness of fit.

Table 5-6. Regression model coefficients and goodness of fit measures

Model	Variable	Coefficients	Standard Error	P-value
	Intercept	-25.18	1.985	< 0.001
	SL	0.80	0.013	< 0.001
	LN	2.61	0.049	< 0.001
	LNW	2.60	0.144	< 0.001
	$RSHD$	3.27	0.063	< 0.001
1	$LSHD$	2.98	0.170	< 0.001
	DN	1.98	0.053	< 0.001
	VEH	-1.83	0.051	< 0.001
	$FEED$	-1.36	0.169	< 0.001
	LOC	1.24	0.151	< 0.001
	R-square		0.39	
Model	**Variable**	**Coefficients**	**Standard Error**	**P-value**
	Intercept	-29.93	1.971	< 0.001
	SL	0.85	0.013	< 0.001
	LNW	2.95	0.145	< 0.001
	$RSHD$	3.26	0.064	< 0.001
2	$LSHD$	2.21	0.170	< 0.001
	DN	1.90	0.054	< 0.001
	$FEED$	-1.43	0.173	< 0.001
	LOC	1.66	0.151	< 0.001
	R-square		0.36	

The models include several predictor variables, so the effects of these variables have an additive contribution to the overall prediction of speed. Although each variable coefficient is evaluated individually, its magnitude is relative to the contribution of information of other variables in the model, so some coefficients may appear to have little impact. Thus, magnitude, sign, p-value, and maintenance of all other variables as fixed were considered for interpretation.

In reference to Model 1, the results of regression modeling indicate that work zone free flow speed increases with an increase in speed limit (SP), lane width, and left/right shy distance to a barrier (LSHD, RSHD). Maintaining all other variables as fixed, vehicles in the left lane travel 2.61 mph faster than those in the right lane. Twelve-foot lanes result in an additional 2.60 mph increase in free flow speed compared to 11 ft lanes. Left and right shy distances to a barrier have similar impacts on free flow work zone speeds, in which an increase of 1 ft in shy distance results in a 2.98 to 3.27 mph increase. Other effects were also quantified in the linear regression model, such as time of the day. The results show that nighttime conditions increase work zone free flow speed by 1.98 mph compared to daytime conditions. The higher speeds at night observed in our data, found to be statistically significant in the linear regression, differ from the findings in the *Highway Capacity Manual* in this regard (TRB 2022). Location 12 had a speed feedback sign in the proximity of the data collection location, so the effect of the feedback sign was found to be statistically significant, with a reduction in speed of 1.36 mph when the sign was present. The location variable (LOC) indicated that, relative to Wisconsin drivers, Michigan drivers had 1.24 mph higher speeds and Illinois drivers had 2.48 mph higher speeds.

Model 2 was developed for practical applications so users can estimate the free flow speed for a work zone based on the speed limit, geometry, day/night, and presence of a speed feedback sign. Essentially, Model 2 does not consider travel lane and vehicle type. The coefficient and trends suggested by Model 2 are similar to those of Model l. Based on Model 2, Figure 5-2 was developed to illustrate the impact of geometric and operational variables such as lane width (LNW), left and right shy distances (LSHD and RSHD), speed limit (SL), daytime conditions, absence of a speed feedback sign, and location in Wisconsin. Figure 5-2 clearly shows that with increasing lane width or shy distance, work zone free flow speeds will increase. It should be noted that in relation to the speed limit, the work zone free flow speed would be 1.7 to 15.0 mph over the speed limit for sites with 12 ft lanes, and speeds would be 1.2 mph below and 12.0 mph above the speed limit for sites with 11 ft lanes. Locations with speed limits between 55 and 60 mph and 1 ft left/right shy distances would experience speeds slightly below the set speed limit.

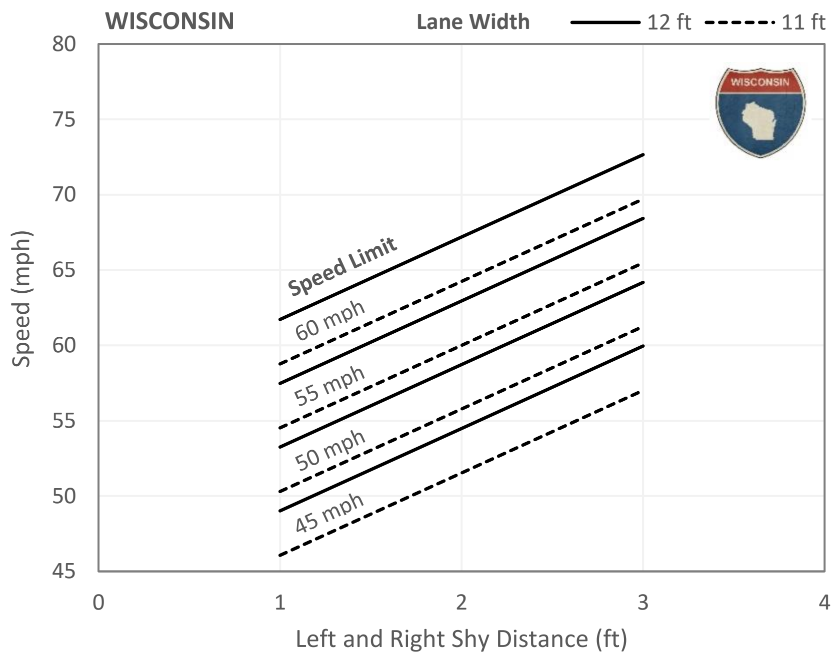

Note: Fixed variables for daytime, no speed feedback sign, and WI conditions

Figure 5-2. Predicted free flow speed for Wisconsin work zones

Figure 5-3 and Figure 5-4 illustrate the impact of geometric and operational variables for Michigan and Illinois, respectively. The lane width and shy distance impacts and other variable impacts are identical to those found for Wisconsin. The only difference is that the model suggests free flow speeds will be higher by 1.66 and 3.32 mph in Michigan and Illinois, respectively.

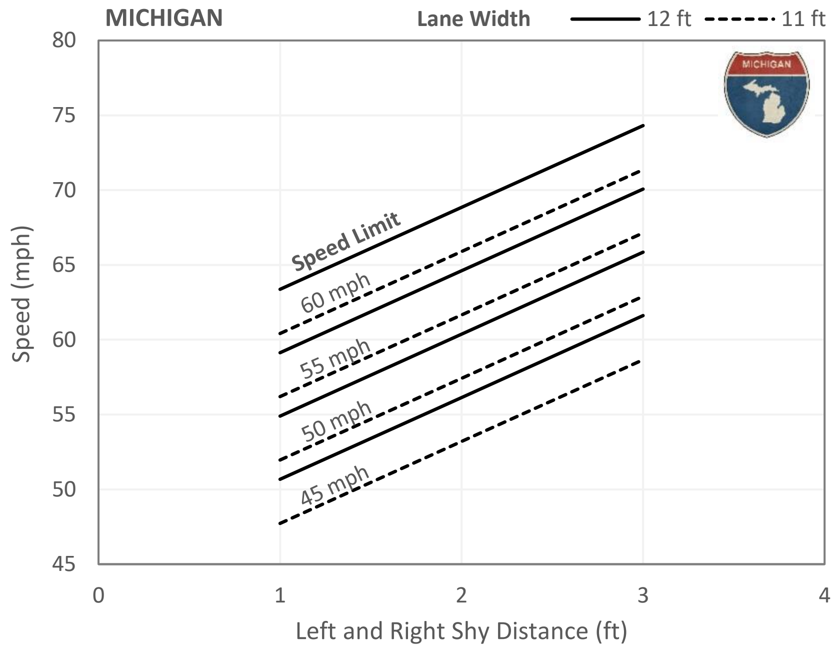

Note: Fixed variables for daytime, no speed feedback sign, and MI conditions

Figure 5-3. Predicted free flow speed for Michigan work zones

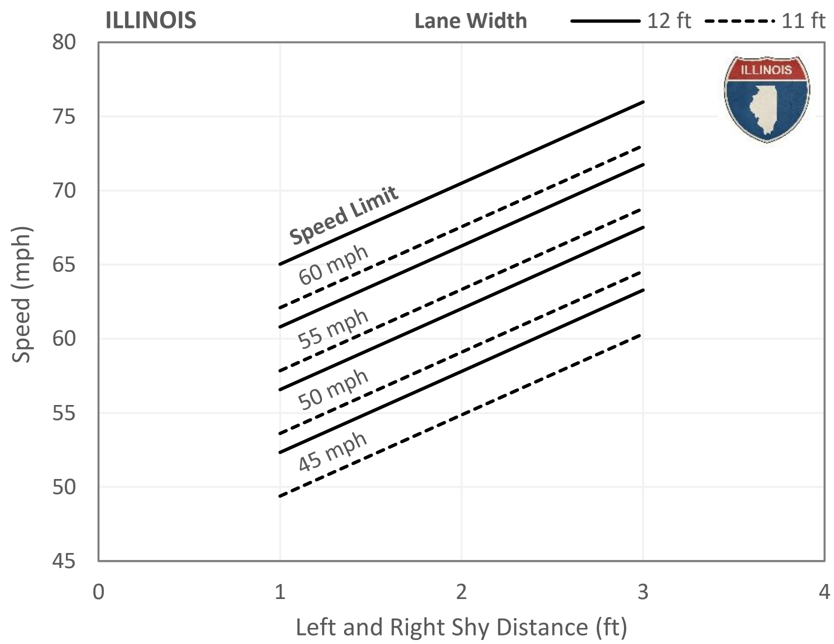

Note: Fixed variables for daytime, no speed feedback sign, and IL conditions

Figure 5-4. Predicted free flow speed for Illinois work zones

5.5. Summary of Mobility Analysis

Free flow vehicle speeds were used to quantify the mobility impacts of lane width and shy distance. Free flow speed data from over 125,000 vehicles were collected at 17 work zone locations in three states. All 17 locations had two lanes open in the work zone. The lane widths were either 11 or 12 ft, and the right shy distances were 1, 2, or 3 ft. Unlike the safety analysis, which only considered vehicles in the right lane, the mobility analysis considered vehicles in both lanes.

An exploratory data analysis of free flow speeds was conducted. Free flow speeds were generally higher in the left lane, as one would expect. Three locations had higher speeds in the right lane. Eleven out of 17 sites showed statistically significant higher speeds during nighttime compared to daytime. This is different from the *Highway Capacity Manual*, which indicates that free flow speeds are greater during the day (TRB 2022). In Wisconsin, the locations with higher speeds at night had lighting. However, a similar correlation between lighting and higher speeds at night could not be found for the Illinois and Michigan locations.

Linear regression modeling was conducted to develop two models for estimating free flow speeds in work zones based on geometric and operational variables. Model 1 is more disaggregate and quantifies the effect of geometric and operational variables, including travel lane and vehicle type. Model 2 uses the same predictors as Model 1 except vehicle type and travel lane. The idea is that Model 2 can be used by work zone designers to estimate free flow speed in work zones at the design stage. Both models indicate similar trends with respect to the impact of the various variables: work zone free flow speed increases with an increase in speed limit, lane width, and left/right shy distance to a barrier. Nighttime free flow speeds are higher than daytime free flow speeds, and speed feedback signs reduce the free flow speeds. Compared to Wisconsin, speeds were higher in Michigan and even higher in Illinois. The research team developed charts illustrating the impact of lane width and shy distance on work zone free flow speeds using the regression models.

As with all research, these findings are subject to limitations. A more uniform distribution of speed limits across the different states would have been preferred. For example, the three Illinois locations had a posted speed of 45 mph, and all of the Michigan locations had a posted speed of 60 mph. Only four locations had a 1 ft shy distance, and all of these were very short sections (a few hundred feet), and that could have impacted the findings. In developing the model, only one location had a speed feedback sign. However, this research demonstrates how speed data can be modeled. Future research efforts should embark on a larger data collection effort to capture greater variability in the different parameters.

6. CASE STUDY

The two previous chapters quantified the safety and speed impacts of lane width and shy distance in two-lane work zones. The objective of this project and the analyses was to enable a comparison between multiple lane width and shy distance configurations for a given paved width. This chapter presents a case study of a 55 mph posted work zone with two open lanes and barriers on both sides with an available paved width of 26 ft. The two geometric configurations are as follows:

1. Lane widths of 12 ft with left and right shy distances of 1 ft
2. Lane widths of 11 ft with left and right shy distances of 2 ft

For speed modeling in this case study, the work zone is assumed to be in Wisconsin, conditions are daytime, and no speed feedback sign is present. The estimated probabilities of edge line encroachment and barrier contact are not affected by day/night. Data and results for the two geometric configurations are provided in Table 6-1.

Table 6-1. Case study configurations and results

Configuration 1	**Value**	**Diagram** (not to scale)
Lane width (LNW)	12 ft	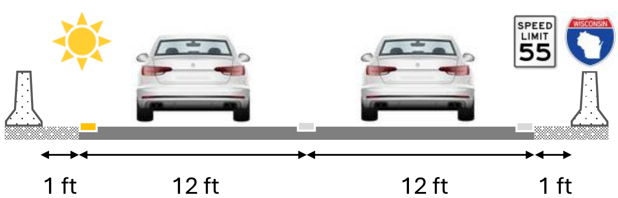
Left/right shy distance (L/RSHD, ft)	1 ft	
Speed limit (SL)	55 mph	
Speed feedback sign (FEED)	Not present	
Time (DN)	Daytime	
State (LOC)	Wisconsin	
Average lateral distance to edge line	50.8 in	
Probability of edge line encroachment	**9.8E-06**	
Average lateral distance to barrier	62.8 in	
Probability of barrier contact	**2.8E-08**	
Estimated free flow speed (SP)	**57.5 mph**	
Configuration 2	**Value**	**Diagram** (not to scale)
Lane width (LNW)	11 ft	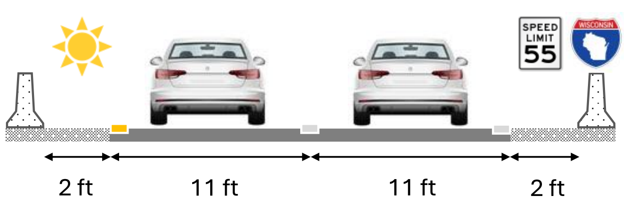
Left/right shy distance (L/RSHD, ft)	2 ft	
Speed limit (SL)	55 mph	
Speed feedback sign (FEED)	Not present	
Time (DN)	Daytime	
State (LOC)	Wisconsin	
Average lateral distance to edge line	35.5 in	
Probability of edge line encroachment	**7.1E-05**	
Average lateral distance to barrier	59.5 in	
Probability of barrier contact	**2.7E-08**	
Estimated free flow speed (SP)	**60.0 mph**	

Under Configuration 1 (12 ft lanes, 1 ft shy distances), vehicles in the right lane are expected to be, on average, 50.8 in. from the right edge line and 62.8 in. from the right barrier. Under

Configuration 2 (11 ft lanes, 2 ft shy distances), vehicles in the right lane are expected to be, on average, 35.5 in. from the right edge line and 59.5 in. from the right barrier. The average lateral distance from the edge line is much greater with a 1 ft shy distance (50.8 in.) than a 2 ft shy distance (35.5 in.). However, the average lateral distances to the right barrier differ by only about 3 in.: 62.8 in. and 59.5 in. under Configurations 1 and 2, respectively. This suggests that the narrow shy distance greatly impacts the lateral distance of vehicles, which shy away from the edge line (and barrier).

The probabilities of edge line encroachment under Configurations 1 and 2 are 9.8E-06 and 7.1 E-05, respectively. In other words, edge line encroachment is about seven times more likely with a 2 ft shy distance than a 1 ft shy distance. While this may appear counterintuitive, this trend is to be expected. Drivers position their vehicles with respect to the barrier. Under narrower shy distances, drivers tend to shy away from the barrier, and it is therefore less likely that they will encroach beyond the edge line. From a safety perspective, the real concern is vehicles making contact with barriers. The probabilities of barrier contact under Configurations 1 and 2 are 2.8 E-08 and 2.7 E-08, respectively, indicating a slightly lower value for Configuration 2. While drivers may veer into the shoulder more with a 2 ft shy distance than with a 1 ft shy distance, the likelihood of contacting the barrier is slightly smaller for a 2 ft shy distance. This illustrates that the EVT approach is able to capture and model the interaction between lane width and shy distance.

The estimated free flow speeds are 57.5 mph and 60.0 mph for Configurations 1 and 2, respectively. In both cases, the free flow speed would be higher than the set speed limit. As stated earlier, to estimate free flow speed, the work zone is assumed to be located in Wisconsin, daytime conditions are present, and speed feedback signs are absent. Free flow speeds would be higher by 3.3 mph in Illinois and 1.7 mph in Michigan, 1.9 mph higher during the night, and 1.4 mph lower with a speed feedback sign.

The results from this case study indicate that Configuration 2 (11 ft lanes, 2 ft shy distance) has a slightly lower probability of barrier contact than Configuration 1 (12 ft lanes, 1 ft shy distance) while having a greater free flow speed. These findings suggest that 11 ft lanes with 2 ft shy distances are better than 12 ft lanes with 1 ft shy distances from the perspectives of safety as well as mobility. While there are limitations for the safety and mobility modeling in this research effort, this finding concurs with existing guidance in the AASHTO Green Book (AASHTO 2018), the *Roadside Design Guide* (AASHTO 2011), and work zone design guidance of multiple states.

7. CONCLUSIONS, LIMITATIONS, AND RECOMMENDATIONS

The goal of this project was to quantify the mobility and safety impacts of different combinations of lane width and shy distance to a barrier for a given paved width. Data from 17 work zone locations across Illinois, Michigan, and Wisconsin were used for the analysis. All 17 locations were in long-term work zones and had two lanes open in the work zone with concrete barriers on either side. The lane widths were either 11 or 12 ft, and the left/right shy distances to the barriers were 1, 2, or 3 ft.

Vehicles' lateral position in the right travel lane was used as a surrogate safety measure to understand the safety impact of lane width and shy distance. Lateral distance data of over a quarter of a million vehicles were used for the safety analysis. The safety analysis only considered right departures for vehicles in the right lane. Lateral distances indicated that, compared to the daytime, vehicles moved farther away from the edge line and barrier in the nighttime. Modeling of all vehicles and tail vehicles (the lowest one percentile of the lateral distance observations) was accomplished by linear regression. Vehicles tended to move farther from the edge line and the barrier in 12 ft lanes compared to 11 ft lanes. All vehicles and tail vehicles tended to gravitate closer to the edge line but farther from the barrier with larger shy distances (3 ft compared to 2 ft and 1 ft). EVT modeling was conducted to estimate the probabilities of right edge line encroachment and right barrier contact. Wider lanes were found to contribute to decreased edge line encroachment and barrier contact, while wider shy distances were associated with increased edge line encroachment and reduced barrier contact.

Free flow vehicle speeds of over 125,000 vehicles were used to understand the mobility impacts of lane width and shy distance. Unlike the safety analysis, which only considered vehicles in the right lane, the mobility analysis considered vehicles in both lanes. Linear regression modeling was conducted to develop two models for estimating free flow speeds in work zones based on geometric and operational variables. Both models indicate similar trends with respect to the impact of the various variables: work zone free flow speed increases with an increase in speed limit, lane width, and left/right shy distance to a barrier. Nighttime free flow speeds were higher than daytime free flow speeds, and speed feedback signs reduced the free flow speeds. Compared to Wisconsin, speeds were higher in Michigan and even higher in Illinois.

A case study of a 55 mph posted work zone with two open lanes in each direction and barriers on both sides was presented. The safety and mobility impacts of two geometric configurations were evaluated: (1) lane widths of 12 ft with left and right shy distances of 1 ft and (2) lane widths of 11 ft with left and right shy distances of 2 ft. The results indicate that Configuration 2 has a slightly lower probability of right barrier contact (for vehicles in the right lane) than Configuration 1 while having a greater free flow speed. These findings suggest that 11 ft lanes with 2 ft shy distances are better than 12 ft lanes with 1 ft shy distances from the perspectives of safety as well as mobility.

As with all research, these findings are subject to limitations. The safety analysis only considered right departures of vehicles in the right lane. Only four locations had a 1 ft shy distance, and all of these were very short sections (a few hundred feet). A more uniform distribution of speed limits across the different states would have been preferred. Only one location had a speed feedback sign.

However, this research has demonstrated how lateral distance and speed data can be modeled. Future research efforts should embark on a larger data collection effort to capture greater variability in the different parameters and to obtain lateral distance from both sides to estimate lane departures in both directions and for vehicles in both lanes.

REFERENCES

AASHTO. 2011. *Roadside Design Guide*. 4th Edition. American Association of State Highway Transportation Officials, Task Force for Roadside Safety, Washington, DC.

AASHTO. 2018. *A Policy on Geometric Design of Highways and Streets*. 7th Edition. American Association of State Highway Transportation Officials, Washington, DC.

Bauer, K. M., D. W. Harwood, W. E. Hughes, and K. R. Richard. 2004. Safety effects of narrow lanes and shoulder-use lanes to increase capacity of urban freeways. *Transportation Research Record*, Vol. 1897, pp. 71–80.

Bham, G. H., and M. A. Mohammadi. 2011. *Evaluation of Work Zone Speed Limits: An Objective and Subjective Analysis of Work Zones in Missouri*. MATC REPORT# 25-1121-0001-119. Mid-America Transportation Center, Lincoln, NE.

Chitturi, M. V., and R. F. Benekohal. 2005). Effect of lane width on speeds of cars and heavy vehicles in work zones. *Transportation Research Record*, Vol. 1920, pp. 41–48.

Coles, S., J. Bawa, L. Trenner, and P. Dorazio. 2001. *An Introduction to Statistical Modeling of Extreme Values*, Vol. 208, p. 208. Springer, London, UK.

Dixon, K., K. Fitzpatrick, R. Avelar, M. Perez, S. Ranft, R. Stevens, and T. Voigt. 2015. *Reducing Lane and Shoulder Width to Permit an Additional Lane on a Freeway*. FHWA/TX-15/0-6811-1. Texas A&M Transportation Institute, College Station, TX.

FHWA. 2004. *Federal Size Regulations for Commercial Motor Vehicles*. U.S. Department of Transportation, Federal Highway Administration, Washington, DC. https://ops.fhwa.dot.gov/freight/publications/size_regs_final_rpt/.

Graham, J. L., R. J. Paulsen, and J. C. Glennon. 1978. Accident analyses of highway construction zones. *Transportation Research Record*, Vol. 693, pp. 25–32.

Gross, F., P. P. Jovanis, and K. Eccles. 2009. Safety effectiveness of lane and shoulder width combinations on rural, two-lane, undivided roads. *Transportation Research Record*, Vol. 2103, pp. 42–49.

Hallmark, S., G. Basulto-Elias, N. Oneyear, O. Smadi, S. Chrysler, and G. Ullman. 2021. *Evaluation of Work Zone Safety Using the SHRP2 Naturalistic Driving Study Data: Volume 2, Description of Research*. Minnesota Department of Transportation, St. Paul, MN.

Mahoney, K. M., R. J. Porter, D. R. Taylor, B. T. Kulakowski, and G. L. Ullman. 2007. *NCHRP Report 581: Design of Construction Work Zones on High Speed Highways*. National Cooperative Highway Research Program, Washington, DC.

Mak, K. K., and D. Sicking. 2003. *NCHRP Report 492: Roadside Safety Analysis Program (RSAP): Engineer's Manual*. National Cooperative Highway Research Program, Washington, DC.

Miaou, S. P. 1997. Estimating vehicle roadside encroachment frequencies by using accident prediction models. *Transportation Research Record*, Vol. 1599. pp. 64–71.

TRB. 2022. *Highway Capacity Manual 7th Edition: A Guide for Multimodal Mobility Analysis*. Transportation Research Board, Washington, DC. https://doi.org/10.17226/26432.

NWSIC. 2019. Work Zone Data. National Work Zone Safety Information Clearinghouse. https://workzonesafety.org/work-zone-data/.

Tarko, A. P. 2012. Use of crash surrogates and exceedance statistics to estimate road safety. *Accident Analysis & Prevention*, Vol. 45, pp. 230–240.

Tarko, A. P., M. Islam, and J. E. Thomaz. 2011. *Improving Safety in High-Speed Work Zones: A Super 70 Study*. FHWA/IN/JTRP-2011/09. Joint Transportation Research Program, Indiana Department of Transportation and Purdue University, West Lafayette, IN.

Urbanik, T., and C. R. Bonilla. 1987. California experience with inside shoulder removals. *Transportation Research Record*, Vol. 1122, pp. 37–46.

APPENDIX: WORK ZONE LOCATIONS

WI-1 10/19/22 Milwaukee URT NB

(a) Viewing downstream

(b) Viewing pavement

WI-2   5/12/23   Mauston   I-90/94 WB CTH N

(a) Viewing upstream

(b) Viewing downstream

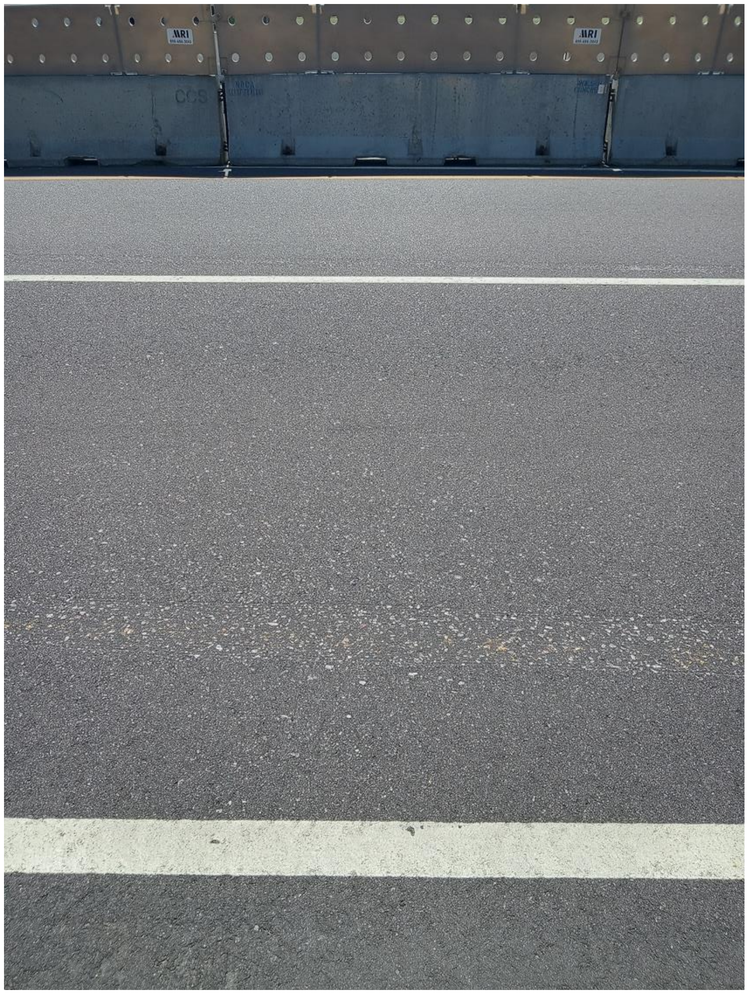

(c) Viewing pavement

WI-3 5/12/23 Mauston I-90/94 WB WI 82

(a) Viewing upstream

(b) Viewing downstream

(c) Viewing pavement

WI-4 5/12/23 Mauston I-90/94 EB CTH G

(a) Viewing upstream

(b) Viewing downstream


(c) Viewing pavement

WI-5 5/16/23 Milwaukee I-43 URT NB

(a) Viewing upstream

(b) Viewing downstream

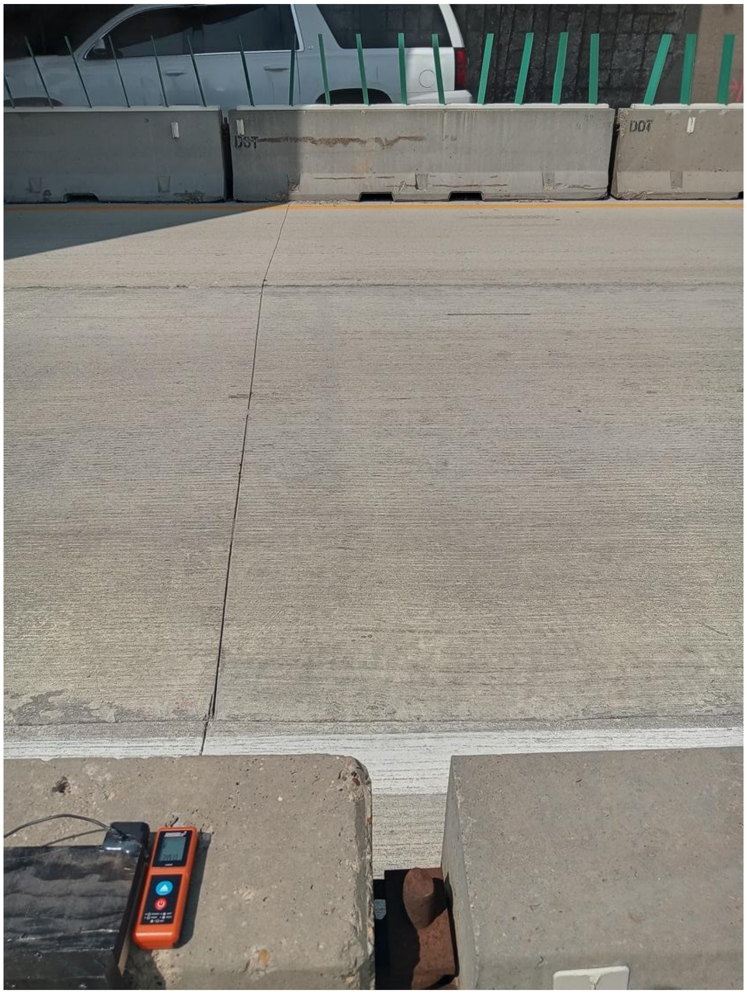

(c) Viewing pavement

WI-6 5/16/23 Milwaukee I-43 EXP NB 89.4

(a) Viewing upstream

(b) Viewing downstream

(c) Viewing pavement

WI-7 5/16/23 Milwaukee I-43 EXP SB STH 60-1

(a) Viewing upstream

(b) Viewing downstream

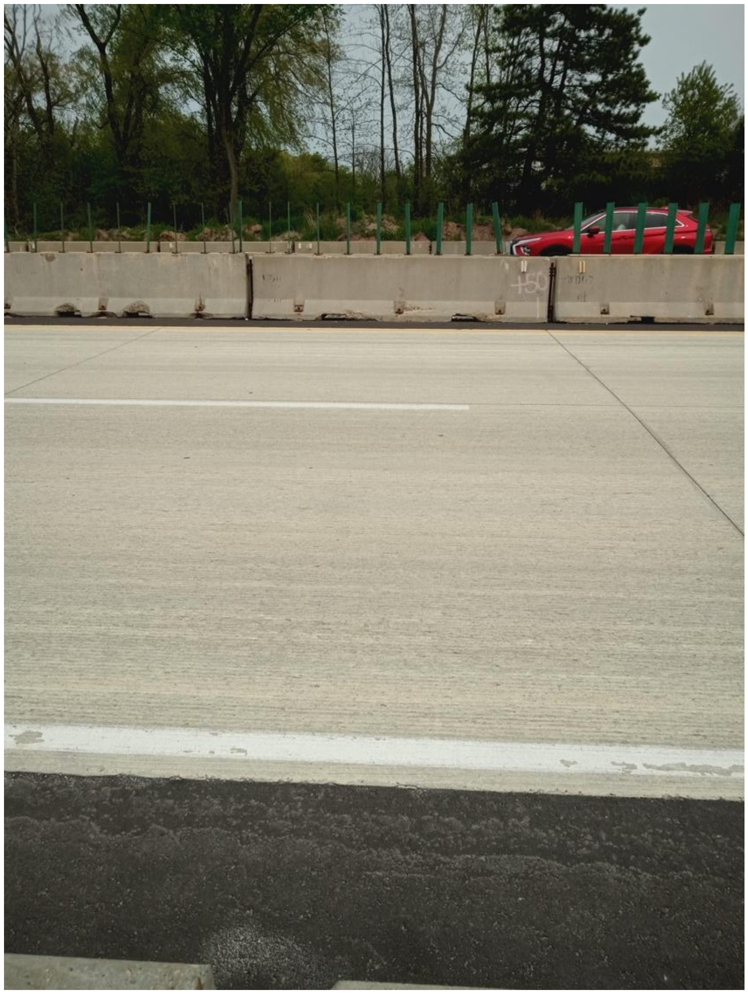

(c) Viewing pavement

WI-8 5/16/23 Milwaukee I-43 EXP SB STH 60-2

(a) Viewing upstream

(b) Viewing downstream


(c) Viewing pavement

MI-1 6/14/23 Detroit I-96 EB Novi

(a) Viewing upstream

(b) Viewing downstream

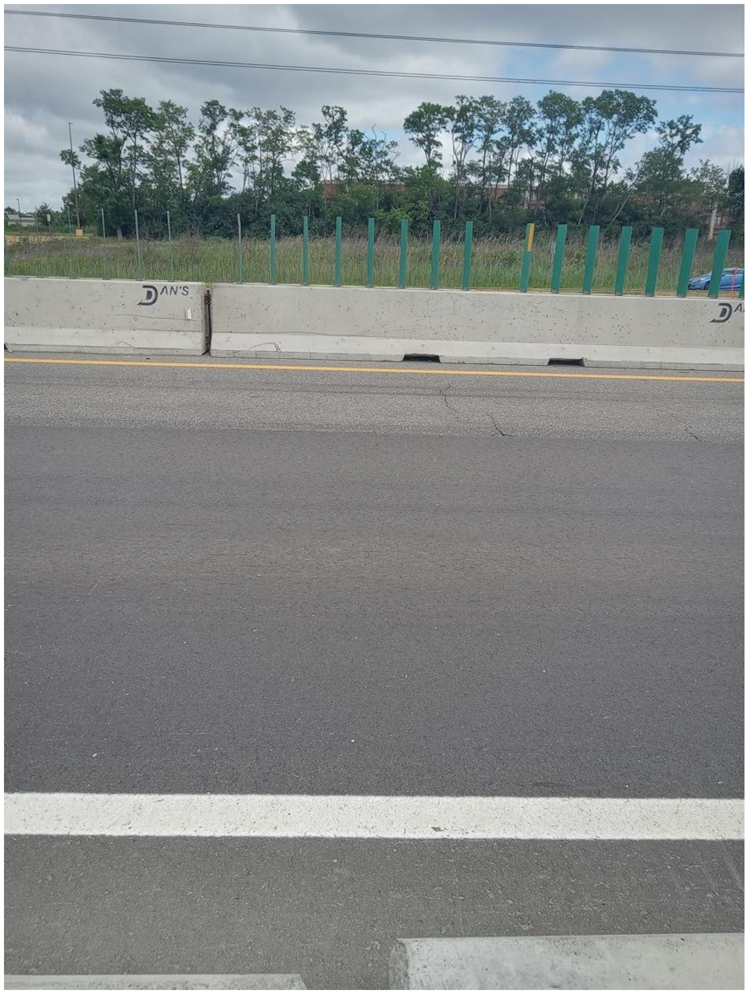

(c) Viewing pavement

MI-2 6/14/23 Detroit I-696 EB Halsted

(a) Viewing upstream

(b) Viewing downstream


(c) Viewing pavement

MI-3 6/14/23 Detroit I-696 EB Farmington

(a) Viewing upstream

(b) Viewing downstream

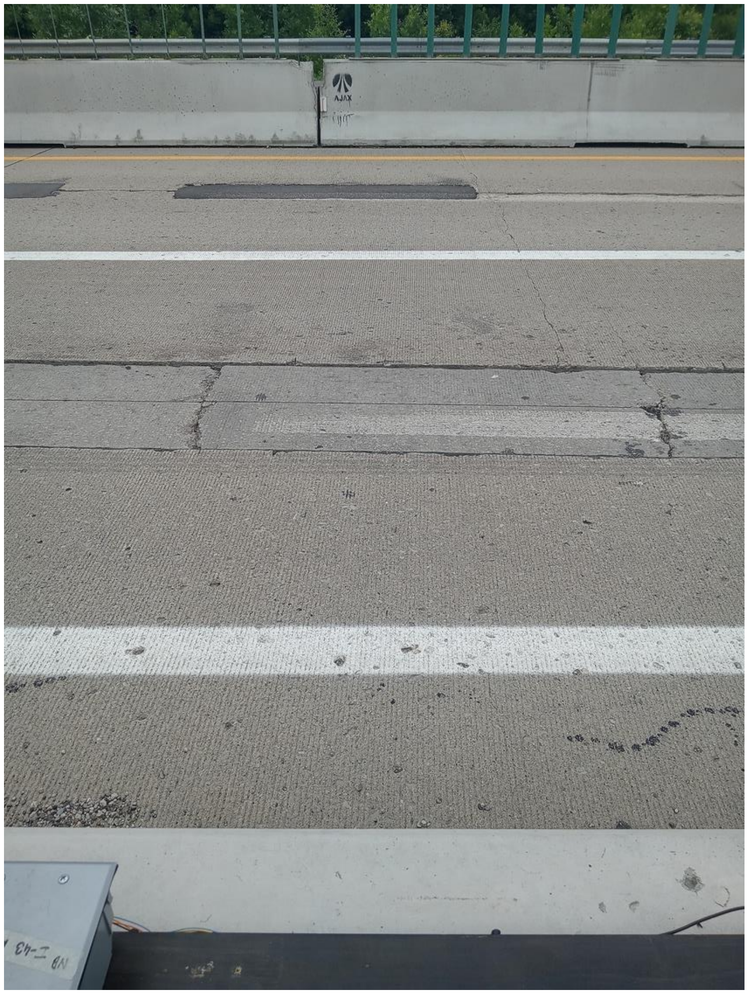

(c) Viewing pavement

MI-4 6/14/23 Detroit I-696 EB Middlebelt-1

(a) Viewing upstream

(b) Viewing downstream

(c) Viewing pavement

MI-5 6/14/23 Detroit I-696 EB Middlebelt-2

(a) Viewing upstream

(b) Viewing downstream

(c) Viewing pavement

MI-6 6/14/23 Detroit I-696 EB Telegraph

(a) Viewing upstream

(b) Viewing downstream

(c) Viewing pavement

IL-1 10/17/23 Joliet I-80 EB Wheeler

(a) Viewing upstream

(b) Viewing downstream

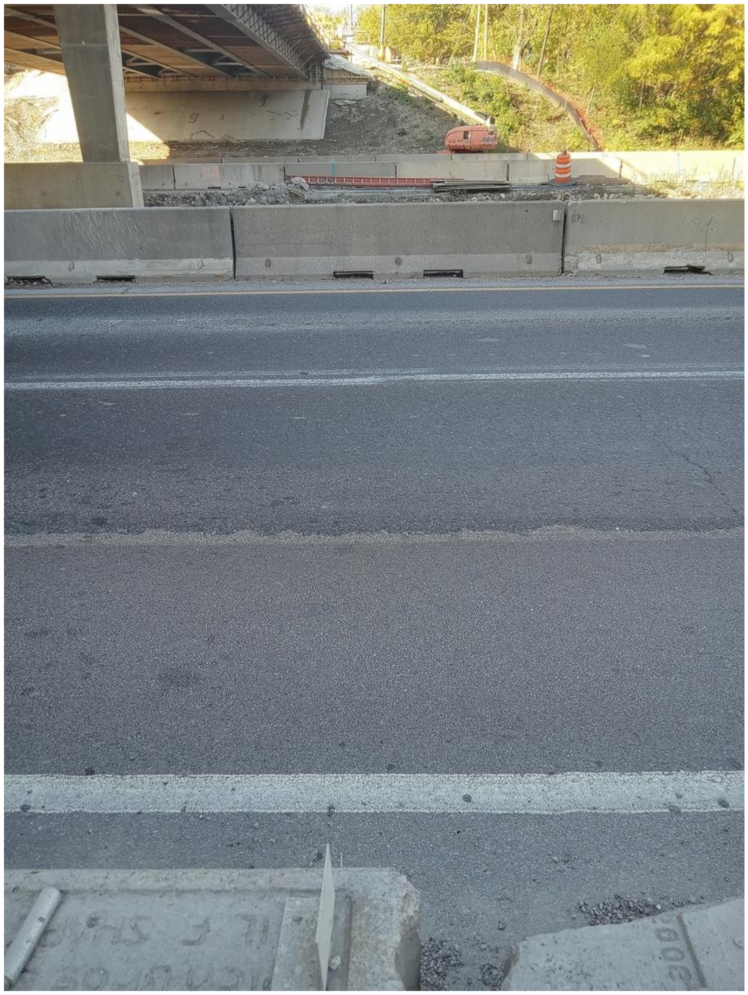

(c) Viewing pavement

IL-2 10/17/23 Joliet I-80 EB Briggs

(a) Viewing upstream

(b) Viewing downstream

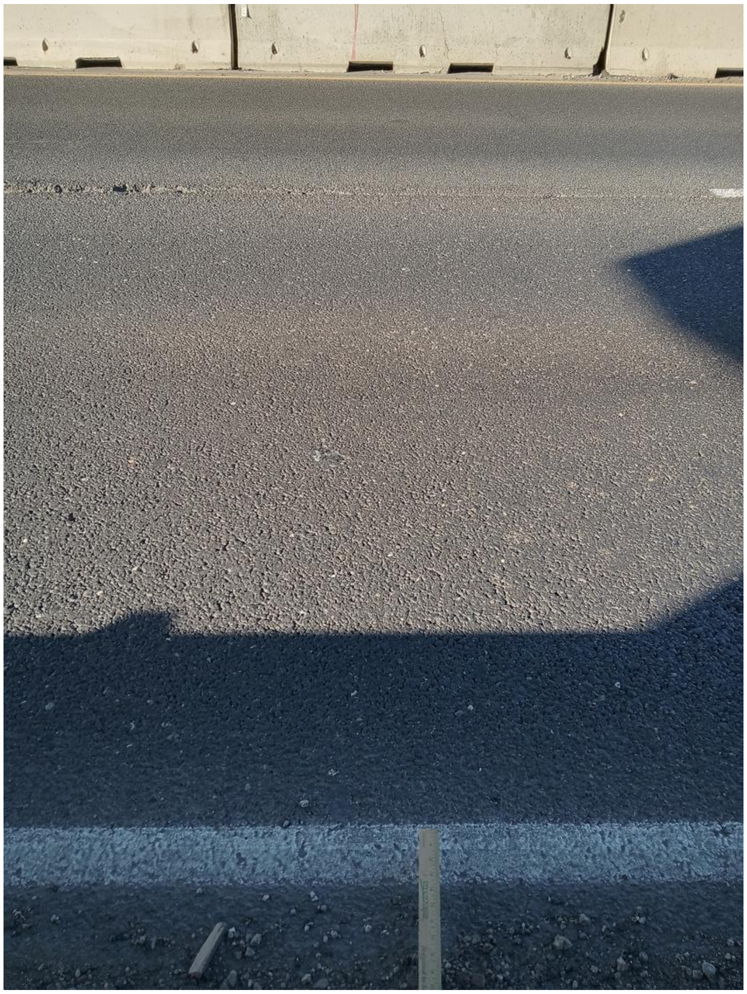

(c) Viewing pavement

IL-3 10/17/23 Joliet I-80 WB Briggs

(a) Viewing upstream

(b) Viewing downstream

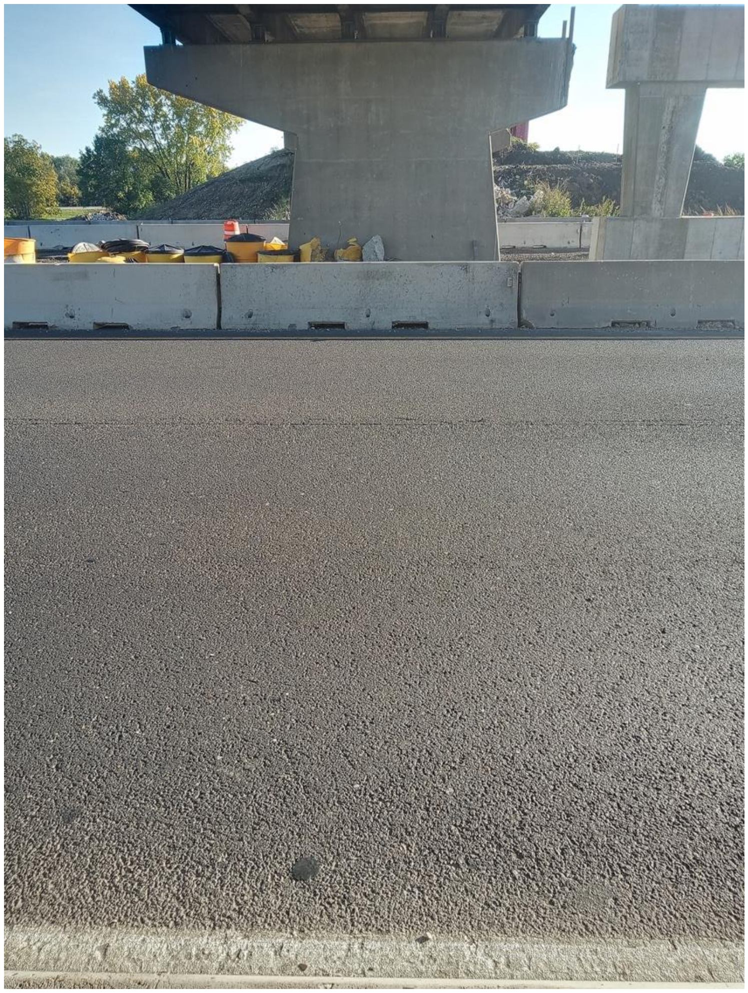
(c) Viewing pavement